

Dear Dr. Herndl,

We are grateful to both reviewers for their thorough assessment of our manuscript. We have modified the paper according to their helpful comments, and we hope that the revised version is now acceptable for publication in Biogeosciences. Below we provide a detailed response to all of the reviewers' comments (in *italics*), indicating the changes that have been made. Line numbers refer to those of the revised manuscript, which includes all tracked changes.

Response to Reviewer 1:

Thank you for your thoughtful and comprehensive critique of our work. We appreciate your insight and attention to detail, and believe the edits made in response to your comments have strengthened our manuscript. We have followed many of your suggestions, including the inclusion of dinoflagellate abundance data, discussion (and statistics) on relative vs. total abundance of different phytoplankton groups, and discussion of the limitations of providing only a subset of process measurements. We also tested additional algorithms (including that of Galí et al. 2018) with some success.

General comments

DMS accounts for approximately 20% of global sulfur emissions and represents a major source of cloud-seeding aerosols in unpolluted marine atmospheres. Therefore, marine DMS emission plays a key climatic role by modulating the radiative properties of aerosols and clouds, as well as precipitation. However, our understanding of DMS drivers across multiple spatial and temporal scales remains limited, and thus our predictive capacity. Reliable high-resolution DMS datasets are essential to improve regional and global DMS climatologies, avoiding artifacts and biases that affect interpolated climatologies based on sparse data, and potentially providing sufficient observations to allow for the evaluation of interannual variability.

The paper by Alysia E. Herr and coauthors makes a valuable contribution to the understanding of DMS distribution patterns in the northeast Subarctic Pacific (NESAP) region. Particularly, it highlights the difficulty in finding unifying criteria across this region, characterized by sharp biogeochemical gradients. From a methodological standpoint, I appreciated the authors presenting traditional discrete GC-FPD measurements along with high-resolution MIMS data (Fig. 3). This comparison increases our confidence in high-resolution DMS surveys, which might be prone to measurement artifacts caused by cell breakage upon pumping and in-line filtration. (I also appreciated the new datasets being readily uploaded to the PMEL archive!). The paper is well written and structured, and the figures and tables are clear and informative. Yet, I suggest the authors to add several citations to give readers a broader perspective on the subject, while recognizing the relevance of previous studies. Below I list what are, in my opinion, the main shortcomings of the article, which I recommend addressing through the Results, Discussion and Conclusions sections:

1. Treatment of DMSPt and phytoplankton groups/size classes in the data analysis. "Dominance vs. abundance":

1.1. I strongly encourage the authors to show total DMSP (DMSPt) concentrations, not just DMSPt:Chl ratios, and analyze their relationship with DMS, simply because DMSPt is the precursor of DMS. DMSPt concentration should be displayed (Fig. 4, 6 and 7).

We have added DMSPp data to Figs. 4, 6, and 7, and have converted DMSPt:Chl to DMSPp:Chl (as per the second referee's request). DMSPd is already included in Figs. 4, 6 and 7, and thus DMSPt can be deduced. We have also examined statistical relationships between DMS, DMSPp and DMSPp:Chl: pg 12, line 2, 26-28; pg 13 line 20-22; pg 14, line 2; pg 45; pg 47-48.

1.2. Correlations between [DMS] and the dominance (relative abundance) of certain phytoplankton groups, as reported in this paper, can be misleading (the same applies to DMS vs. the DMSPt:Chl ratios). For example, in transect T3 (Fig. 7), the authors report a negative correlation between DMS and relative prymnesiophyte abundance ($r = -0.75$). In the middle of T3, inshore of the front, Chl increases sharply from ~ 1 to $30 \mu\text{g L}^{-1}$, whereas % prymnesiophytes decreases from $\sim 20\%$ to $\sim 5\%$. Still, the abundance of prymnesiophytes increases by about 8-fold, while DMS increases "only" by ~ 3 -fold (~ 5 to ~ 15 nM). Thus, the increase in prymnesiophytes might suffice to explain the increase in DMS, be it through direct DMS release by prymnesiophytes or through the activity of micrograzers and bacteria. It is well known that increases in microphytoplankton abundance (mostly diatoms) are generally accompanied by increases of other phytoplankton groups (Barber and Hiscock, 2006; Uitz et al., 2006), as in the current dataset.

Thank you for pointing this out. We calculated total abundance of various phytoplankton groups and found no correlations between DMS and total prymnesiophyte and dinoflagellate abundance. Along T3, correlation between DMS and total diatom abundance remained quite high. We have included discussion and some statistics regarding this point: pg 18, line 1-7.

1.3 Dinoflagellates: Why is their abundance not reported and their role not discussed, although they are quoted in the Introduction and beginning of the Discussion as important players (Steiner et al., 2012)? More generally, I wonder what phytoplankton groups made up the $\sim 50\%$ of the pigment biomass that is omitted in Fig. 4, 6 and 7. What about other high-DMSP nanophytoplankton like chrysophytes and pelagophytes?

We initially did not include dinoflagellate data, as this group represented only a minor proportion ($<10\%$) of phytoplankton across our study area. In the revised article, we now discuss the relationship between DMS and the combined relative abundance of prymnesiophytes and dinoflagellates. In general, results from this modified analysis are very similar to those obtained from a prymnesiophyte-only approach, with increased correlation coefficients in some cases: pg 11, line 33; pg 13, line 3; pg 14, line 1.

We have also included more data regarding other phytoplankton groups, including green algae, picoeukaryotes and prokaryotes: pg 11, line 26; pg 12, line 29-30; pg 13, line 30-31.

As our HPLC-derived estimates were somewhat limited with regards to taxa specificity, we unfortunately do not have information on the abundance of chrysophytes or pelagophytes.

2. Process measurements:

2.1. I was puzzled to see dissolved DMSP consumption rate constants (kDMSPd) ranging between ~ 30 and 100 d^{-1} , while kDMSPd values in the literature are generally lower than 10 d^{-1} (Galí and Simó, 2015). Highest kDMSPd reported so far are $\sim 20 \text{ d}^{-1}$ in the NE Pacific (Royer et al., 2010) and near South Zealand (Lizotte et al., 2017). Is there a mistake? Everything would look more consistent in terms of S and C cycling (Kiene and Linn, 2000) if the reported kDMSPd had units of h^{-1} instead of d^{-1} . Otherwise, the contribution of heterotrophic DMSPd consumption to DMSPt cycling and bacterial S and C demand would be suspiciously high (as some quick calculations can show).

The rate constants for DMSPd turnover were indeed high in the study area, and they are, in fact, among the highest measured anywhere. These measurements were made by Ron Kiene's group, one of the world-leaders in this area. Ron carefully examined the raw data and was confident that the measurements are robust. (The reviewer may know that Ron tragically passed away very recently). The very high rate constants were observed were likely due, in part, to the high productivity waters sampled, as well as some methodological modifications that minimized release of DMSPd during the ^{35}S -DMSP tracer incubations. We now briefly mention these factors in our revised discussion: pg 5, line 30; pg 20, line 4-5.

2.2. Although the data suggest distinct DMS(P) cycling regimes, I am not sure the amount of process measurements suffices to resolve DMS variability across fronts. In addition, important DMS production and loss terms were not measured. The finding that variations in biological DMS consumption (kDMS) drove [DMS] across regions seems robust (although DMS photolysis, a potentially important loss term, was not measured). Regarding DMS sources, DMS production from particulate DMSP cleavage was not assessed, and previous studies suggest it is important globally (Galí and Simó, 2015) and in this region (Asher et al., 2017). This fits well with prymnesiophyte and (dinoflagellate?) driven DMS production.

As DMS concentration is set by the dynamic balance between gross production rates (nM d^{-1}) and total DMS loss rate constants (d^{-1}) (Galí and Simó, 2015), conclusions based on a subset of production and loss processes are weak. Note also that the contribution of DMSPd turnover to DMS concentration is set by the product $[\text{DMSPd}] \cdot \text{kDMSPd} \cdot \text{Yd}$, where Yd is the DMS yield from dissolved DMSPd consumption. Thus, the relationship between kDMSPd and [DMS] tells little if Yd is not known (Yd can easily vary between 5 and 20%). The control of kDMS on [DMS] is comparatively more direct. I propose:

(i) displaying the relationship between kDMS, [DMS] and potentially other variables (T, S, Chl, ...) in a scatterplot-like graphic.

(ii) discussing more in depth the control of [DMS] by measured and non-measured DMS budget terms to give a more balanced view of the potential processes at play (see Galí and Simó, 2015).

This is a fair point. To address it, we now discuss the limitations of the conclusions we can draw from our data, acknowledging the lack of measurement of several important terms: pg 19, lines 4-10.

We made some scatter plots, as suggested by the reviewer, but these plots only showed the moderate linear relationship between $kDMS$ and $[DMS]$, with no particular trend based on temperature, salinity, etc., thus adding little information.

3. Algorithm evaluation and regional tuning:

Several previous studies have shown that global-scale algorithms have poor skill at predicting regional DMS variability (e.g. Bell et al., 2006; Galí et al., 2018; Hind et al., 2011), not to talk about the mesoscale. The authors tried to tune pre-existing algorithms to their dataset using least squares fits, but they did not show the new coefficients, only the improved skill metrics. Consequently, the interpretation of this exercise remains vague and does not shed much light on the controlling factors, nor it helps designing better algorithms. I suggest either deleting this section (my choice) or reshaping and expanding it to make it more informative (making use of the supplemental information).

We have clarified our discussion of algorithm results, and also included results from the new Galí et al., 2018 algorithm (see responses below): pg 15, lines 29-34; pg 22, lines 7-14.

Coefficients for each algorithm were recalculated for each region tested, resulting in 16 sets of coefficients. Since these regionally-tuned algorithms performed poorly, we see little utility in reporting them.

Specific comments

Introduction

P2 L17: please specify what zone of the "Southern Ocean". Iron-depleted regions of the subpolar Southern Ocean (approx. 40 to 60S) are relatively unproductive and typically have low $[DMS]$... (Jarníková and Tortell, 2016; Kiene et al., 2007; Lana et al., 2011).

Done: pg 2, line 16-17

P3 L1-7: These lines suggest that we do understand what causes high DMS concentrations in this area. I think we don't, for two main reasons:

(i) We do not understand interannual variability (Galí et al., 2018; Steiner et al., 2012). (ii) We do not understand well enough the interplay between iron limitation, dominance of high DMSP producers (depicted by $DMSPt:Chl$) and DMS production pathways. The authors quote "the effects of mixed layer stratification and Fe-limitation, which may act to increase DMS/P production as a means to offset oxidative stress (Sunda et al. 2002)". However, Royer et al. (2010) found a positive correlation between iron concentration and $DMSPt:Chl$ ratios in the HNLC area within the NESAP. This is contrary to what one would expect if Fe stress caused major increases in $DMSPt:Chl$ ratios. It is possible that small Fe additions stimulate preferentially high DMSP producers (Levasseur et al., 2006; Steiner et al., 2012), which would result in a positive correlation between $DMSPt:Chl$ and Fe as long as high DMSP producers are

not outcompeted by diatoms. Regarding DMSP- to-DMS yields, although Royer et al. (2010) documented higher bacterial DMS yields in the Fe-depleted HNLC region, Steiner et al. (2012) pointed to dinoflagellates and micrograzers as key players in DMS production. The latter would imply a dominant role of DMS production from the particulate pool, involving phytoplanktonic DMSP lyases. These processes are poorly documented in the NESAP area.

We have added some additional text clarifying the role of Fe limitation in driving DMS/P dynamics in the Subarctic Pacific: pg 3, lines 13-17.

P3 L12: I suggest citing here Simó et al. (2018) (The quantitative role of microzooplankton grazing in dimethylsulfide (DMS) production in the NW Mediterranean) to support the importance of grazing-mediated DMS production. A major finding of that paper is that "throughout the year, grazing-mediated DMS production explained 73% of the variance in the DMS concentration".

Thank you for this suggestion. We have now cited this paper: pg 3, line 12..

P3 L18. I missed two relevant citations here:

1. Belviso et al. (2003) "Mesoscale features of surface water DMSP and DMS concentrations in the Atlantic Ocean off Morocco and in the Mediterranean Sea". A precursor study showing sharp changes in DMS:DMSPt:Chl across mesoscale features and fronts.
2. Royer et al. (2015) Small-scale variability patterns of DMS and phytoplankton in surface waters of the "tropical and subtropical Atlantic, Indian, and Pacific Oceans". A high-resolution DMS survey across 21000 km in the tropical oceans, showing that "much of the variability in DMS concentrations occurs at scales between 15 and 50 km, that is, at the lower edge of mesoscale dynamics, decreasing with latitude and productivity. DMS variability was found to be more commonly related to that of phytoplankton-related variables than to that of physical variables".

Thank you, added: pg 3, lines 21-22.

Methods

P5 L3: Please report more statistics (RMSE, mean bias, linear regression equation...) comparing MIMS and GC-FPD, either here or on the figure (which should be 3, not 2).

Done: pg 5, lines 4-5.

P6 L27: Phytoplankton biomass tends to peak in late summer in the oceanic sector of the NESAP. Regarding DMS, there seems to be more similarity between August and September than between August and June (Galí et al., 2018; Lana et al., 2011; Steiner et al., 2012), perhaps related to the dinoflagellate abundance in late summer (Steiner et al., 2012). I understand the authors' choice reflects data availability, but I suggest cautioning the reader that June, July and August can be very different.

We have clarified a sentence justifying our choice of JJA for the summer climatology, while acknowledging the point raised by the reviewer: pg 6, line 33; pg 7, lines 1-2..

P7 L14-15: Please add citations for all satellite products: PAR (Frouin et al., 2003), Chl-a (Hu et al., 2012; O'Reilly et al., 1998).

Done, thank you: pg 7, lines 19-20.

P7 L29: What fraction of your 1-degree bins is over bottom depths shallower than 2000 m, where MLD is not available? Could this bias the evaluation of empirical algorithms, given the distinct biogeochemical dynamics of shelf seas? What would be the impact of replacing time-resolved MLD data by a monthly climatology? Perhaps using climatological MLD would make a little difference in oceanic areas, while allowing testing of the algorithms in the entire NESAP domain. Also, how did data gaps caused by cloudiness affect algorithm evaluation? (as suggested by P9 L25 in Results, and Fig. 1 top panels).

We have added information regarding % of MLD coverage: pg 8, lines 1-2.

We did indeed assess the utility of using a number of different MLD climatologies. (We actually assessed empirical algorithms and pairwise regressions using climatologies of all variables). However, in no case did a monthly MLD climatology yield a stronger relationship with DMS. We chose to consistently use time-matched data rather than mixing approaches.

P7 L30: Please specify what DMS and SST datasets were used in combination with daily 2.5-degree wind speed data to calculate DMS flux: non-binned data, 1-degree binned data retaining temporal variability, or the 1-degree summer climatology?

Reworded for clarity: pg 8, lines 7-9.

P8 L9: I would add "all observations within the JJA months for a given year were averaged" (to avoid confusion with the way monthly climatologies like L11 are calculated).

Done: pg 8, lines 16-17.

P8 L27: Did you try Spearman's rank correlations? This could help identifying nonlinear monotonic relationships.

Yes. However, results were only minimally different than Pearson's correlation coefficients, and in no case revealed substantially stronger relationships.

P8 L32: If the section on algorithm evaluation is not dropped, the authors could also evaluate the two-step algorithm of Galí et al. (2018). We showed that it outperforms SD02 and VS07 in most oceanic areas, although it has difficulties to reproduce the DMS seasonal cycle at Ocean Station P. The global algorithm of Anderson et al. (2001) would also be an interesting choice here as it performed well across contrasting trophic regimes in the SE Pacific (Hind et al., 2011).

Based on these suggestions, we evaluated and included results from Galí et al. (2018), and found that it was able to reproduce DMS with reasonably good accuracy in the CCAL province. We expanded our discussion based on these results, and compared them to the negative correlations found using the VS07 algorithm: pg 15, lines 29-34; pg 22, lines 7-14.

We tested the algorithm of Anderson et al. (2001), and found that it performed very poorly across all areas.

Results

P10 L10-15: How well compare the estimates of phytoplankton size classes derived from absorption (underway WetLabs instrument) to HPLC pigments?

We have now addressed this in the Methods section: pg 5, lines 13-14.

P10 L18: The difference may be significant due to large N, but is it relevant when the ranges overlap so much? Note also that saying DMS concentrations were significantly different in different years downplays the utility of calculating a multiyear climatology.

This is a good point. We have deleted this sentence.

P11 L12: Beyond the high SSHA-DMS coherence at the mesoscale, Fig. 5 shows there is a lot of unresolved submesoscale variability, probably due to biological heterogeneity, in agreement with (Royer et al., 2015).

We have addressed this in the discussion: pg 17, line 26-27.

P11 L20: Relative abundance or absolute? Also, I suggest specifying that these size classes were derived from underway absorption data, not HPLC, to avoid confusion.

Done: pg 11, line 30.

P11 L30: How can significance be tested with $n = 2$ at each side of the front (Fig. 4)? I suggest reporting ranges. Qualitatively, I agree that k 's were different at either side of the front.

We have changed wording to report this as a qualitative result, with insufficient sampling to allow for statistical testing: pg 12, line 7-8.

P12 L1-2: This explanation is unclear. See general comment 2.2.

P12 L31-32: Same as above.

We have clarified the wording here: pg 12, lines 12-13 and addressed the subject in discussion: pg 19, lines 4-10.

P13 L30: Can this be tested statistically somehow? See general comment 2.2.

Too few data points for reliable statistics. We have changed wording to report this as a qualitative result: pg 14, line 6.

P13 L33: Please check units (general comment 2.1).

Units OK (see response to general comment 2.1).

P15 L15-26: See general comment 3. This section would be more interesting if the authors explained the rationale behind the original algorithms, reported the tuned coefficients, and explained in what sense they alter the performance of the original algorithms. In particular, turning from negative to positive slope in VS07 completely alters the rationale behind this algorithm.

This phenomenon and the rationale behind this algorithm is now addressed in the revised discussion: pg 22, lines 7-14.

Discussion

P17 L13: could you please explain more explicitly the relationship between positive SSHA and high DMS? Eg, anticyclonic eddies detaching from a frontal area and transporting a certain water type, or whatever... This can help us understand why SSHA can show both positive and negative correlations to DMS (as explained at the bottom of the same page).

Done: pg 17, lines 25-37.

P17 L19: The unpublished meta-analysis should be cited as pers. comm., I guess.

This paper is now published and the citation has been updated: pg 17, line 32.

P17 L23-27: The negative correlation between SRD and DMS in the whole region (Table 5, original VS07 algorithm) goes against this argument.

Addressed in discussion: pg 22, lines 7-14.

P18 L20: OK, but transient [DMS] and kDMS do not even need to be invoked. The relationship may also arise at nearly-steady state, where $[DMS] = (\text{gross production rate}) / (\text{total loss rate constant})$, where total loss is dominated by biological DMS consumption k , as explained by (Galí and Simó, 2015).

We feel that the original wording is clear, and in keeping with the manner that results are presented by the subsequently cited studies.

P18 L26: As the authors explain, DMS consumption rates will be positively correlated to [DMS] as long as [DMS] is more variable than kDMS, because $\text{cons. rate} = [DMS] * kDMS$. I suggest removing this sentence.: "In contrast to DMS rate constants (d^{-1}), water column DMS consumption rates ($nM d^{-1}$) showed a positive correlation with DMS concentrations ($r=0.65$,

p=0.01). This result is not unexpected, as consumption rates are the product of rate constants and in situ concentrations".

Done.

P19 L4: I also suggest removing this: "In contrast to biological loss, turnover time due to sea-air flux showed no correlation to DMS concentrations".

Done.

P19 L13-23: I suggest refining the writing here: see general comment 2.2.

We have added discussion addressing the limitations of basing conclusions on a subset of rate measurement data: pg 19, lines 4 – 10.

P19 section 4.4: Would it be possible to quantify interannual variability of DMS (see Fig. 3 of Steiner et al., 2012) using the merged dataset? Interannual variability has been overlooked (Galí et al., 2018), with so much emphasis on the mean (climatological) state... This part of the Discussion is currently a bit poor.

Only 18/216 grid cells contained at least 5 years of data, and many of these were not contiguous. Thus, little information could be gleaned from this approach.

P20-21, section 4.6: The last two paragraphs of this section seem to contradict each other. Does elevated productivity (which usually follows elevated biomass) translate into high DMS, or not? If only in some places, why? What are the relevant scales for this comparison? It would be interesting to cite here the work of (Kameyama et al., 2013) "Strong relationship between dimethyl sulfide and net community production in the western subarctic Pacific", perhaps extracting more information from your own NCP vs. DMS data.

This is addressed further in section 4.7: pg 22, lines 7-14.

P21 L17-18: Data from tables 4 and 5 supports this idea, so I suggest citing the tables here (ie, the HNCL PSAE shows the highest negative correlations between DMS and bot NO₃ and SRD).

Added citation for table 5, but not table 4, as the relationship between DMS and NO₃ in the PSAE is not significant: pg 22, line 8.

Edits

P5 L5-6: I suggest removing "and rate measurements to examine potential drivers of spatial variation". Rates were not measured in underway samples...

Reworded for clarity: pg 5, line 7.

P6 L12: "sampled" should be "samples".

Done: pg 6, line 16.

Table 1: please replace "June" by "August" for cruise LPA07.

Done: pg 37

P12 L7-8: please remove "given no new production". DMS removal expressed as a daily % would also hold in the presence of DMS production (as it is usually the case).

Done.

P15 L1: Please correct "We also calculated and DMS:Chla..." P20 L14: "distinction", rather than "measure"?

Done: pg 21, line 3.

Response to Reviewer #2,

Thank you for your thoughtful critique of our work, and the suggestion of many helpful references. We have followed your suggestions in many places, including the conversion of bacterial productivity data to carbon units, inclusion of DMSPp data, and discussion of previous studies from areas outside of the NESAP.

Interactive comment on "Patterns and drivers of dimethylsulfide concentration in the northeast Subarctic Pacific across multiple spatial and temporal scales" by Alysia E. Herr et al. As the title indicates, this manuscript describes DMS and DMSP spatial and temporal distribution patterns with high-resolution field data collected in coastal waters of the NE Pacific. The DMS patterns are compared to historical field data in a publicly available database, collected mostly in previous decades and further offshore. Measurements of some of the rates involved in DMS cycling allow for interpretation and discussion of the likely controls (or drivers) of the next patterns observed. No single physical or biological parameter accounted for the DMS/P variability observed and described as a whole in the region; rather probable controls change in relative importance within subregions, as has been shown in other studies. This variability only confirms the already described complexity of the DMS/P/O biogeochemical system at any one place and time. The manuscript is very well written and is a pleasure to read. However, the authors should decide whether they will focus this report on the NE Pacific ONLY and hence solely references for this region will be used. Right now, the manuscript ignores many references to similar conclusions in other regions or even in nearby SE Bering Sea (Barnard et al.) while occasionally using references from other regions to support its own conclusions (eg. North Sea,

Southern Ocean). The authors miss a unique chance to strengthen the conclusions of this manuscript.

Page: 3 -Line 1: what is L11? Lana et al. 2011? Please check throughout ms

We have now defined this acronym at first appearance: pg 2, line 14

-Line 18: Holligan et al 1987 first reported the link between DMS and fronts; even if it was not in NESAP waters but NAtlantic waters .

We added this reference and others: pg 3, line 21-22

Page: 6 -line 7: Please report BP data in carbon units, not leucine units so they can be compared with PP data and with other studies.

Done: pg 6, line 9-10; Fig. 4, 6, 7

-Line 8: Hence, as done previously by Kiene et al, DMSPp can be estimated such that the DMSP/chl ratios are estimated with both parameters in the particulate fraction; only makes a difference where and when [DMSPd] are high. Fig 4 shows a match for DMSPt and DMSPd measurements; hence, DMSPp can be calculated.

We have added DMSPp values to figures: pg 6, line 12-13; Fig. 4, 6, 7

-line 9: with a GC-FPD discrete method

Added: pg 6, line 10-11

-line 12: sampleS

Corrected: pg 6, line 16

-line 15: "The estimation formulas" used?

Corrected: pg 6, line 20

Page: 7 -line 6: where were the SSS and SST matches obtained from? The PMEL data set does not provide them.

Nearly all PMEL data for this region provides matched SSS and SST. The percentage of DMS data obtained from this source with matched SSS and SST values has been added: pg 7, lines 10-11.

Page: 8 -line 21-22: I had come to assume that L11= Lana et al 2011. If yes, please reword this sentence

Corrected: pg 8, line 31

-line 23: please insert "The PMEL" data were first...

Corrected: pg 8, line 31

-line 32: replace 'that' with 'those'

Corrected: pg 9, line 9

Page: 10 -similar DMS/P-NPP relationship by Bell et al for the North and South Atlantic along the AMT transect and by Matrai et al for the Barents Sea. Should be addressed in the Discussion.

This is a relatively minor result based on our high resolution underway data. We did not include this topic in the discussion, as we believe it would dilute our discussion of contrasting DMS cycling regimes.

Page: 11 -2nd paragraph: because similar conclusions of prymeniophytes vs other phyto groups and DMS/P patterns were drawn by Barnard et al 1984? in the SE Bering Sea, they should be definitively mentioned in the Discussion.

Thank you for pointing out this oversight. We have added a reference to this study on pg 17, line 5, and point out the similar results directly on pg 17, line 35; pg 18, line 1.

Page: 15 -line 1: something is missing before 'and'; or remove 'and'; or replace by 'a'?

Corrected: pg 15, line 11.

Page: 16 -section 4.1 and elsewhere: Since references beyond the NESAP are already included, other -mostly older- very pertinent references have been suggested in this review and should be included to strengthen the arguments made.

-line 11: but not in polar waters (Turner et al for southern ocean; Matrai et al for Barents Sea)

Have added references: pg 16, line 19.

line 13: please insert after 'physiological state' "as previously shown by Gabric et al. (1999)" [Barents Sea]

Done: pg 16, line 22.

-line 14: please insert 'e.g.' in front of the refs listed, as there are other pertinent refs as well

Done: pg 16, line 23

-line 27: please insert 'and elsewhere' after NESAP

Done: pg 17, line 5

-line 31: which studies? add references!

Done: pg 17, line 5

Page: 17 -line 6: waterS

Corrected: pg 17, line 16

-somewhere in this page: A similar conclusion on the influence of prymensiophytes in 3 coastal domains just a bit north in the NE Pacific was reported by Barnard et al 1984. Please include.

Done: pg 17, line 35; pg 18, line 1..

-line 19: update the McParland and Levine ref, as the ms has moved on in its review process –

Corrected: pg 17, line 32

-line 26, after the Sunda et al. 2002 ref. Please address the observation that a post-bloom = also when bacterial activity is highest and DMSPd > DMSPp, as phyto cells become leakier (eg, Matrai and Keller 1993 and Malin et al 1993 for cocco blooms; Stefels et al review as well)

We have now added some brief discussion of this: pg 18, lines 17-19

Page: 18 -line 3: add a few references after ‘cell lysis’ for all processes mentioned -line 6: instead and/or in addition to the variables reported herein? -line 8: which ‘studies’? add refs (e.g., xxx)

Done: pg 18, lines 12-14

-line 9: is this only for coastal waters of the NESAP? Or elsewhere also? Please specify. This is not a new observation for other regions (e.g., Turner et al Southern Ocean, Matrai et al. Barents Sea)

Done: pg 18, lines 31-32

-line 21: please insert “in other regions” after ‘previous studies’!

Done: pg 19, line 18

-line 29: please insert “in other regions” after ‘previous studies’

Done: pg 19, line 24

-line 31-32: check punctuation

Reworded: pg 19, 26-27

Page: 19 -line 2: please convert to carbon units!

Done: pg 19, line 29

-line 7: it IS possible

Corrected: pg 19, line 32

-line 21-23: delete this paragraph. It is naive and does not add anything

Done.

Page: 20 -section 4.5: Both Hind et al 2011 and Deutsch et al 2009 in the Eastern SPacific and globally, respectively, combined Longhurst provinces and DMS-based algorithms to test their predictions. Both studies should be referenced and included here as they discussed the strengths and weaknesses of such DMS predictive algorithms. Hind et al. also include many of the variables discussed in this study, even the presence of eddies and upwelling.

We have included the reference to Hind. Perhaps the reviewer is referring to the paper by Derevianko et al. 2009, on which Deutch was an author. This paper examines model performance, but does not include Longhurst provinces (it is a global study). We have added two other papers that do utilize provinces (Belviso et al. 2011, and Royer et al. 2015): pg 19, line 2.

Page: 22 -line 1: supportS

This section was otherwise edited based on the other referee's comments.

-line 1: please insert "in summer" after 'hotspots'

Done: pg 22, line 31

-line 10: By US NSF rules, shouldn't all data be submitted to a long-term data repository? .

We have the data prepared for submission to the PMEL data server. However, the site is currently unavailable due to the partial US government shut-down. These data included paired ancillary variables.

Page: 24-32 References -check subscripts and italics for scientific names throughout -format references; remove all caps throughout

Corrected.

Page: 34 -please insert “(in parenthesis)” at the end of the Table 2 title. That’s what is in (xxx), right?

Corrected (should be clear what’s in parentheses now): pg 38, lines 2-3.

Page: 41 -Fig 4d y-axis: why not DMSPp/chl a? both are particle-bound variables These are discrete stations.

We have now changed this to DMSPp/chl a : pg 45, line 4

-Fig 4f: can you please report BP in Carbon units? otherwise it cannot be compared with PP or other studies

Corrected: pg 45

Page: 42 -Fig 5: the y-axis scale is missing

Corrected: pg 46

Page: 43 -same comments as for Fig 4

Page: 44 -same comments as for Fig 4

Corrected: pg 47, 48

Page: 46 -Fig 9: Given the tables, fig 8 and the fact that the differences in the DMS flux estimates is so small, this figure does not add much and could be removed

We have chosen to keep this figure, as it demonstrates areas where concentrations vary significantly from PMEL data.

1 **Patterns and drivers of dimethylsulfide concentration in the northeast** 2 **Subarctic Pacific across multiple spatial and temporal scales**

3 Alysia E. Herr¹, Ronald P. Kiene², John W. H. Dacey³, Philippe D. Tortell^{1,4}

4 ¹Department of Earth, Ocean and Atmospheric Sciences, University of British Columbia, Vancouver, BC, V6T 1Z4, Canada

5 ²Department of Marine Sciences, University of South Alabama, Mobile, AL, 36688, USA

6 ³Woods Hole Oceanographic Institute, Woods Hole, MA, 02543, USA

7 ⁴Department of Botany, University of British Columbia, Vancouver, BC, V6T 1Z4, Canada

8 *Correspondence to:* Alysia E. Herr (aherr@eoas.ubc.ca)

9 **Abstract.**

10

11 The northeast subarctic Pacific (NESAP) is a globally important source of the climate-active gas dimethylsulfide (DMS), yet
12 the processes driving DMS variability across this region are poorly understood. Here we examine the spatial distribution of
13 DMS at various spatial scales in contrasting oceanographic regimes of the NESAP. We present new high spatial resolution
14 measurements of DMS across hydrographic frontal zones along the British Columbia continental shelf, together with key
15 environmental variables and biological rate measurements. We combine these new data with existing observations to produce
16 a revised summertime DMS climatology for the NESAP, yielding a broader context for our sub-mesoscale process studies.
17 Our results demonstrate sharp DMS concentration gradients across hydrographic frontal zones, and suggest the presence of
18 two distinct DMS cycling regimes in the NESAP, corresponding to microphytoplankton-dominated waters along the
19 continental shelf, and nanoplankton-dominated waters in the cross-shelf transitional zone. DMS concentrations across the
20 continental shelf transition (range <1–10 nM, mean 3.9 nM) exhibited positive correlations to salinity ($r=0.80$), sea surface
21 height anomaly (SSHA; $r=0.51$) and the relative abundance of prymnesiophyte and dinoflagellates ($r=0.89$). In contrast, DMS
22 concentrations in near shore coastal transects (range <1–24 nM, mean 6.1 nM) showed a negative correlation with salinity ($r=-$
23 0.69 , $r=-0.78$) and SSHA ($r=-0.81$, $r=-0.75$), and a positive correlation to relative diatom abundance ($r=0.88$, $r=0.86$). These
24 results highlight the importance of bloom-driven DMS production in continental shelf waters of this region, and the role of
25 prymnesiophytes and dinoflagellates in DMS cycling further offshore. In all areas, the rate of DMS consumption appeared to
26 be an important control on observed concentration gradients, with higher DMS consumption rate constants associated with
27 lower DMS concentrations. We compiled a dataset of all available summertime DMS observations for the NESAP (including
28 previously unpublished results) to examine the performance of several existing algorithms to predict regional DMS
29 concentrations. None of these existing algorithms was able to accurately reproduce observed DMS distributions across the
30 NESAP, although performance was improved by the use of regionally tuned-coefficients. Based on our compiled observations,
31 we derived an average summertime distribution map for DMS concentrations and sea–air fluxes across the NESAP, estimating
32 a mean regional flux of 0.30 Tg of DMS-derived sulfur to the atmosphere during the summer season.

1 **1 Introduction**

2 Spurred by a proposed role in climate regulation as a source of cloud-condensation nuclei and back-scattering aerosols, the
3 biogenic trace gas dimethylsulfide (DMS) and related organic sulfur compounds dimethylsulfoniopropionate (DMSP) and
4 dimethyl sulfoxide (DMSO) have been studied for more than four decades (Lovelock et al. 1972; Charlson et al. 1987). This
5 body of research has revealed complex sulfur biogeochemical cycling in the oceans, and important physiological and
6 ecological roles for these molecules (Simó 2004; Stefels et al. 2007). DMSP and DMS have been shown to play an essential
7 function in marine microbial systems as sources of carbon and sulfur (Kiene et al. 2000; Reisch et al. 2011). These molecules
8 also act as olfactory foraging cues for numerous species of birds, fish, marine invertebrates and mammals (Seymour et al.
9 2010; Johnson et al. 2016), thereby driving interactions both within and beyond the marine microbial food web. The ecological,
10 chemical and climatological significance of DMS and related compounds has stimulated significant effort to understand the
11 surface ocean distribution of these molecules and the underlying factors driving their variability.

12

13 The Pacific Marine Environmental Laboratory (PMEL) has compiled a database of over 47,000 discrete DMS measurements.
14 Lana et al. (2011, [hereafter L11](#)) utilized these data to construct a global climatology of surface ocean DMS concentrations
15 and sea–air fluxes, providing broad-scale understanding of oceanic distribution patterns. The global mean DMS concentration
16 is estimated to be approximately 2 nM, but the climatology reveals several regional ‘hot spots’ of elevated DMS accumulation,
17 including polynya waters of the Southern Ocean, and [the](#) northeast Subarctic Pacific (NESAP). In these regions, surface ocean
18 DMS concentrations 5–10-fold higher than the mean oceanic value are commonly observed (Kiene et al., 2007; Lana et al.
19 2011, Jarníková and Tortell 2016). Although large-scale global patterns derived from the climatology are likely robust, a fuller
20 understanding of spatial and temporal patterns of regional DMS variability is constrained by the relatively poor spatial and
21 temporal coverage of existing measurements.

22

23 The NESAP, defined here as the region bounded by 44.5° N and 61° N latitude and 180° W and 120° W, exhibits consistently
24 high summertime DMS concentrations in both open ocean and coastal regions, with maxima of ~20 nM observed during the
25 late summer season (Wong et al. 2005; Asher et al. 2011, 2017; Steiner et al. 2012). This oceanic region is also characterized
26 by strong spatial heterogeneity of environmental characteristics. High-productivity coastal upwelling regions transition to iron-
27 limited high nutrient low chlorophyll (HNLC) waters offshore (Boyd and Harrison 1999; Boyd et al. 2004). Seasonally varying
28 surface currents, fresh water inputs, coastal upwelling and recurrent formation of westward-propagating mesoscale eddies
29 result in semi-permanent and transient hydrographic frontal zones, impacting regional marine biodiversity and productivity
30 (Crawford et al. 2005; Whitney et al. 2005; Ribalet et al. 2010). This spatial heterogeneity makes it challenging to quantify
31 DMS distributions from discrete ship-based sampling, and complicates region-wide generalizations of DMS dynamics.

32

33 Recent work has highlighted differences in the distribution of DMS and related compounds across distinct domains of the
34 NESAP, particularly in offshore and coastal regions (Wong et al. 2005; Asher et al. 2011, 2017; Steiner et al. 2012). The
35 HNLC offshore region was identified by L11 as an area of high DMS concentrations and sea–air fluxes. Results from in situ

1 observations (Wong et al. 2005; Levasseur et al. 2006; Merzouk et al. 2006; Asher et al. 2011) and numerical models (Steiner
2 et al. 2012) suggest that elevated DMS concentrations in these open ocean waters are driven by the presence of high DMS/P
3 producing phytoplankton taxa, such as prymnesiophytes and dinoflagellates, and the effects of mixed layer stratification and
4 Fe-limitation, which may act to increase DMS/P production as a means to offset oxidative stress (Sunda et al. 2002, [Kinsey et
5 al. 2016](#)). A low particulate [organic](#) carbon to sulfur ratio in the HNLC regime further influences bacterial DMSP metabolism,
6 resulting in increased DMS-yield from DMSP metabolism (Merzouk et al. 2006; Royer et al. 2010). In the physically dynamic
7 coastal waters of the NESAP, high DMS concentrations likely result, in part, from seasonal coastal upwelling, which drives
8 high phytoplankton biomass accumulation. [Recent work](#) (Asher et al. 2017) has demonstrated an enhancement of DMS
9 accumulation following upwelling events [in the coastal NESAP](#), consistent with previously observed high DMS/P
10 concentrations in [other](#) upwelling regions (Hatton et al. 1998; Zindler et al. 2012; Wu et al. 2017). Increased DMS
11 concentrations in the post-upwelling bloom phase may result from nitrogen limitation, increased grazing pressure (which
12 releases DMSP into the dissolved pool; [Simó et al. 2018](#)), oxidative stress associated with shoaling mixed layers, and a
13 phytoplankton community shift towards high DMSP-producing species (Nemcek et al. 2008; Franklin et al. 2009). [Despite
14 these advances in understanding DMS dynamics in the NESAP, many aspects of DMS cycling in this region remain poorly
15 documented, including the factors influencing interannual variability \(Steiner et al., 2012; Galí et al., 2018\), the interplay
16 between iron concentration and phytoplankton community shifts \(Levasseur et al. 2006; Roayer et al. 2010\), and the relative
17 importance of phytoplanktonic DMSP lyases and micrograzers \(Steiner et al. 2012\).](#)

18
19 New advances in sensor technology over the past decade have begun to significantly expand DMS data coverage in a number
20 of ocean regions. These fine scale measurements reveal novel features and highlight the apparent influence of oceanographic
21 frontal zones in driving fine-scale DMS distribution patterns ([Holligan et al. 1987](#); [Locarnini et al. 1998](#); [Belviso et al. 2003](#);
22 [Tortell 2005a](#); [Nemcek et al. 2008](#); [Royer et al. 2015](#); Jarníková et al. 2018). In previous work (Asher et al. 2017), we have
23 documented sharp transitions in DMS concentrations across salinity frontal zones in nearshore NESAP waters. This earlier
24 work did not include corresponding measurements of DMS/P turnover rates, limiting mechanistic interpretation of the observed
25 spatial patterns. To our knowledge, there has been no systematic evaluation of the processes driving fine-scale DMS variability
26 across frontal zones. Such a study requires high resolution concentration measurements together with assessments of
27 biological productivity and DMS/P turnover rates.

28
29 In this article, we present a new data set of DMS/P concentrations across coastal and open ocean waters of the Subarctic
30 Pacific, from the northern Gulf of Alaska to the Oregon coast. Using a suite of measurements collected during two summer
31 cruises (2016–2017), we document regional-scale features, and characterize sub-mesoscale DMS structure across
32 hydrographic frontal zones in on-shelf and transition regions. Using real-time ship-board measurements, we were able to
33 select contrasting sites across frontal zones for more extensive sampling and analysis, allowing us to probe underlying rate
34 processes in adjacent areas [with distinct](#) DMS/P concentrations and surface water hydrography. We combined our new data
35 set with existing observations from our own group and from the existing PMEL database to produce a new summertime DMS

1 climatology for the NESAP. This updated climatology enables us to better constrain the summertime distribution of DMS in
2 the NESAP, identifying persistent ‘hot spots’, and exploring correlations between DMS concentration and other biotic and
3 abiotic variables. We also use our compiled data set to evaluate various empirical algorithms predicting DMS concentrations
4 and sea–air fluxes across the NESAP. Our results yield new insights into the spatial patterns and potential drivers of
5 summertime NESAP DMS distribution across various spatial scales in a globally important oceanic region.

6 **2 Methods**

7 **2.1 Data overview**

8 In this study, we combined new data from two recent oceanographic expeditions with existing observations derived from
9 several decades of compiled DMS measurements in the NESAP. Ancillary measurements of various environmental and
10 biological variables were obtained from a number of sources (ship-based measurements, remote sensing and blended data
11 products) to help interpret DMS distribution patterns. The various data sets are described below.

12 **2.2 New high-resolution data sets**

13 **2.2.1 Underway ship-board measurements**

14 Field sampling was conducted on board the University–National Oceanographic Laboratory System (UNOLS) vessel *Oceanus*
15 during July of 2016 and August of 2017 (O16, O17, respectively). Our cruise tracks included offshore, coastal and transitional
16 waters throughout the Gulf of Alaska (Fig. 1). We define the coastal regime as those waters with bottom depths shallower
17 than 2000 m, following Asher et al. (2011). We utilized real-time DMS measurements (see below) and NASA satellite ocean
18 colour imagery (AquaMODIS) to guide our cruise track, enabling us to identify areas with high concentrations of DMS and
19 strong spatial gradients in surface water phytoplankton biomass and hydrography (sea surface temperature and salinity).
20 During O16 we also conducted detailed surveys of three hydrographic frontal zones that exhibited sharp DMS concentration
21 gradients. One of these surveys (T1; Fig. 1) was located in the coastal-open ocean transition near Dixon Entrance north of
22 Haida Gwaii (formerly the Queen Charlotte Islands), while the other two transects were located along the British Columbia
23 continental shelf (T2: Hecate Strait and T3: La Perouse Bank; Fig. 1). After an initial survey to examine frontal structure,
24 stations were selected for depth-resolved sampling to cover the gradients present across the frontal zone. The O17 cruise
25 covered a similar area as O16. Although we did not perform detailed transect surveys on this second cruise, we did sample
26 waters near T1–T3.

27

28 High resolution surface water DMS measurements were conducted using membrane inlet mass spectrometry (MIMS)
29 following published methods (Tortell 2005b; Nemcek et al. 2008). The MIMS system, sampling from the ship’s underway
30 seawater flow through system (~5 m intake depth), allows for high-frequency measurements (2–3 times per minute), yielding
31 a spatial resolution of ~150–200 m at normal ship speeds of 8–10 kts. During these cruises, DMS concentrations were also

1 measured in discrete water samples collected at 5 m depth using a purge-and-trap system connected to a gas chromatograph
2 equipped with a flame-photometric detector (FPD-GC) (Kiene and Service 1991). These discrete measurements were used to
3 assess the accuracy of MIMS-based measurements. We found good agreement between methods, with a mean absolute error
4 of 0.90 nM, [root mean square error of 1.4 nM, and coefficient of determination of \$r^2=0.89\$](#) between the two instruments across
5 the full range of measured concentrations (Fig. 3).

6
7 High resolution DMS measurements were paired with [rate measurements and](#) ancillary underway data to examine potential
8 drivers of spatial variation. A [ship](#)-board thermosalinograph was used to measure sea surface temperature (SST) and salinity
9 at high spatial resolution (SBE 45 and SBE 38 for salinity and temperature, respectively). Chlorophyll-*a* (chl-*a*) concentration
10 was measured using a WET labs ACS absorbance/attenuation meter, based on the absorption line height at 676 nm (Bricaud
11 et al. 1995; Roesler and Barnard 2013; Burt et al. 2018). These chl-*a* concentrations were further used to derive an estimate
12 of phytoplankton [assemblage size structure](#) and taxonomic distributions, based on the empirical algorithm of Hirata et al.
13 (2011). [Phytoplankton size-class estimates derived from this algorithm agreed well \(\$r^2 > 0.75\$ \) with discrete HPLC-derived](#)
14 [estimates](#) (methods described below; Zeng et al. 2018). MIMS was also used to determine the ratio of oxygen and argon
15 concentrations relative to atmospheric saturation. The resulting biological oxygen saturation term, $\Delta O_2/Ar$, can be used to
16 calculate net community productivity (NCP) from the air–sea gas exchange of O_2 (Kaiser et al. 2005). We used the calculation
17 approach of Reuer et al. (2007) to compute NCP from our $\Delta O_2/Ar$ measurements. We note that some of these estimates,
18 particularly in regions of active upwelling, are likely [negatively](#) biased by the entrainment of O_2 under-saturated water into the
19 mixed layer. While this effect can be accounted for using N_2O measurements (Izett et al. 2018), we do not have these data
20 available for our cruises. Our derived NCP estimates thus likely represent under-estimates, and we have removed all negative
21 NCP values. Nonetheless, the general spatial patterns we observed in NCP are likely to be robust.

22 2.2.2 Station-based measurements

23 We measured a suite of variables at selected sampling stations along the cruise track. All water for ancillary measurements
24 was taken from 5 m depth, collected using Niskin bottles. A Seabird CTD probe (Seabird 911plus) was deployed at each
25 station to obtain depth profiles of hydrographic features over the upper 200 m of the water column. A density difference
26 criterion of 0.05 kg m^{-3} was used to calculate mixed layer depths.

27
28 DMS loss and DMSP consumption rates were measured using the radio-labeled ^{35}S methods outlined by Kiene and Linn (2000)
29 [with some modifications to minimize the release of DMSPd during incubations](#). Briefly, ^{35}S -labeled DMSPd or DMS were
30 added to samples at non-perturbing concentrations ($<1\%$ of ambient levels). Samples were incubated in the dark at surface
31 water temperatures for $<1 \text{ h}$ (^{35}S -DMSP) or $<7 \text{ h}$ (^{35}S -DMS). The rate constant for DMSPd turnover was determined by
32 measuring the disappearance of ^{35}S -DMSP from the dissolved ($< 0.2 \mu\text{m}$) pool. The rate constants for DMS loss were
33 determined by measuring the accumulation of dissolved, non-volatile ^{35}S transformation products [derived from](#) the volatile

1 ³⁵S-DMS tracer. Consumption rates (nmol L⁻¹ d⁻¹) were calculated by multiplying in situ DMS or DMSPd concentrations by
2 the measured rate constant (k_{DMS} or k_{DMSPd} respectively).

3
4 Primary productivity was measured using 24 h ¹⁴C uptake incubations, following the method outlined by Schuback et al.
5 (2015). Incubation bottles were held in a deck-board incubator plumbed with continuously flowing seawater to achieve in situ
6 temperature. The light intensity was adjusted to ~ 30 % surface irradiance enriched in blue light using neutral density screening
7 in combination with blue photographic film (LEE filters: #209 and CT blue maximum transmission at approximately 460 nm).
8 Light levels in the tank were measured with a ULM-500 light meter equipped with a 4π-sensor (Walz). Bacterial production
9 was measured using the tritiated leucine method (Smith and Azam 1992) [and converted to carbon units \(Simon and Azam](#)
10 [1989; Ducklow et al. 2000\)](#). Station samples were also [analysed](#) for total and dissolved DMSP (DMSPt and DMSPd) [with a](#)
11 [GC-FPD discrete method](#) using the previously described NaOH cleavage and small-volume gravity drip filtration method
12 (Dacey and Blough 1987; Kiene and Slezak 2006). [DMSPp was calculated by subtracting DMSPd from DMSPt \(Zindler et](#)
13 [al. 2012, Levine et al. 2016\)](#).

14
15 We obtained discrete estimates of phytoplankton assemblage composition using diagnostic pigment analysis (DPA) of
16 photosynthetic pigments measured using HPLC. For these measurements, 1 L samples were collected on GF/F filters (nominal
17 pore size ~ 0.7 μm), flash frozen in liquid nitrogen and stored frozen until analysis [at the NASA Goddard Space Flight Center](#)
18 [Ocean Ecology Laboratory \(Van Heukelem and Thomas 2001\)](#). The DPA method was originally developed by Vidussi et al.
19 (2001), and subsequently refined (Uitz et al. 2006; Hirata et al. 2008; Brewin et al. 2010) to more accurately capture
20 phytoplankton type and size class. The estimation formulas [used](#) here are those of Hirata et al. (2011), [with coefficients tuned](#)
21 [specifically for the NESAP by Zeng et al. \(2018\)](#). Percent contribution to phytoplankton assemblage was assessed for three
22 size classes (micro, nano, and pico).

23 **2.3 Compilation of published data**

24 To provide a broader regional spatial context for our observations, we combined discrete DMS measurements from the PMEL
25 data archive with high spatial resolution DMS measurements made using MIMS since the early 2000s. Table 1 provides dates
26 and spatial domains of the cruises, along with relevant literature citations. Note that some of the DMS data included in this
27 compilation have not been previously published. All of our compiled MIMS data have been made available on the PMEL
28 database (<https://saga.pmel.noaa.gov/dms/>).

29 **2.3.1 MIMS data sets**

30 MIMS-based observations included in this study are derived from 11 cruises conducted between 2004 and 2017, primarily
31 aboard the Canadian Coast Guard Ship *John P. Tully* as part of ongoing time-series monitoring programs conducted by the
32 Department of Fisheries and Oceans Canada (DFO). Only summertime data (defined here as June, July and August; [JJA](#))
33 falling within the NESAP region (44.5°–61° N, 180°–120° W) were included in this compilation. [Although DMS](#)

1 [concentrations and phytoplankton biomass often remains high through September \(Galí et al., 2018; Lana et al., 2011; Steiner](#)
2 [et al., 2012\)](#), [there are fewer DMS data available for this month.](#) Measurements were binned to a temporal sampling resolution
3 of 1 minute. All DMS data points are paired with shipboard sea surface salinity and SST. The cruises VIJ04, VIJ10, WCAC10,
4 LPA11, O16 and O17 [also](#) include paired NCP [estimates](#) obtained from MIMS measurements, using the $\Delta\text{O}_2/\text{Ar}$ -based method
5 described above.

6 **2.3.2 PMEL data extraction**

7 We accessed the PMEL data base (<http://saga.pmel.noaa.gov/dms/>) on 6 December, 2017 to extract observations from June,
8 July and August in the NESAP region defined above. Our selection criteria yielded 3236 data points between 1984 and 2003.
9 These observations were relatively evenly distributed between the three months, but were biased spatially, with a
10 preponderance of data derived from on-shelf waters off the coast of Alaska (see Fig. 8b). [As with MIMS data, the majority of](#)
11 [data points in the PMEL data base](#) included paired sea surface salinity and SST measurements [\(94.6% and 99.8%, respectively\).](#)

12 **2.4 Ancillary measurements**

13 Ancillary oceanographic data were used to contextualize DMS spatial distributions, examine potential correlations to
14 environmental variables and evaluate the performance of several empirical algorithms predicting DMS concentrations. In
15 many cases, ancillary variables of interest (e.g. chl-*a*) were not reported in conjunction with DMS data, and we thus utilized a
16 number of remote sensing data products, as described below. Remotely-sensed parameters were linearly interpolated to the
17 spatial resolution of ship-based DMS observations.

18
19 AquaMODIS satellite data were used to obtain information on photosynthetically available radiation (PAR; [Frouin et al. 2003](#)),
20 chl-*a* (OCI algorithm; [O'Reilly et al. 1998; Hu et al. 2012](#)), calcite (Gordon et al. 2001; Balch et al. 2005) and diffuse
21 attenuation coefficients (Werdell and Bailey 2005). For these data products, we extracted level 3 gridded data from
22 <http://oceancolor.gsfc.nasa.gov/cgi/l3> at 9 km resolution. Monthly means for chl-*a*, calcite and k_d were utilized to maximize
23 spatial coverage [by minimizing data gaps caused by cloudiness](#), whereas 8 day average PAR data were used. AquaMODIS
24 chlorophyll [and sea surface temperature \(SST\) data](#) were also used to [estimate](#) sea surface nitrate (SSN) using a North Pacific-
25 specific algorithm (Goes et al. 2000). Aqua MODIS data are only available starting in July of 2002, whereas most of the
26 PMEL data set in this region is from sampling prior to 2003. For earlier observations [\(going back to 1997\)](#), we used chl-*a* data
27 from the SeaWiFS satellite. [Satellite chl-*a*, calcite and \$k_d\$ data were unavailable for data prior to 1997 \(<1% of DMS data\).](#)

28
29 We obtained information on sea-surface height anomalies (SSHA) using gridded data sets (5 day, $0.17^\circ \times 0.17^\circ$ resolution)
30 obtained from ftp://podaac-ftp.jpl.nasa.gov/allData/merged_alt/L4/cdr_grid_interim. This level 4 satellite product is derived
31 from various sensors, and data are not available before 1992. Mixed layer depths at a monthly, 1° resolution were obtained
32 from the China Second Institute of Oceanography (CSIO) ftp://data.argo.org.cn/pub/ARGO/BOA_Argo/. These data are based
33 on gridded Argo float data [interpolated](#) using the Barnes method, and are available for the years 2004–present (Li et al. 2017).

1 Due to limitations in Argo operational depths, data are largely absent from waters shallower than 2000 m ([136 out of 249 1° x](#)
2 [1° bins](#)).
3

4 We calculated sea–air DMS fluxes from DMS concentration data and surface wind-speeds using the gas transfer
5 parameterization of Sweeney et al. (2007) and the Schmidt number formulation of Saltzman et al. (1993). Wind speed data
6 for flux calculations were obtained from the NCEP/NCAR reanalysis dataset
7 (<https://www.esrl.noaa.gov/psd/data/gridded/data.ncep.reanalysis.pressure.html>) at a 2.5° daily resolution. [These calculations](#)
8 [were performed prior to data binning \(described below\), such that temporally-resolved sea–air flux was calculated for all](#)
9 [~150,000 DMS data points](#). Following previous studies, we assume negligible atmospheric DMS concentrations for our
10 calculations, leading to a potential (though likely small) overestimate of the sea–air flux. For purposes of comparison to fluxes,
11 we calculated DMS column burden along transects by multiplying DMS concentration and average mixed layer depth.

12 2.5 Data binning and province assignment

13 High resolution, underway measurements may introduce sampling biases due the large number of data points collected. For
14 example, a ship holding station will increase spatial data density at a particular location, and the large number of observations
15 can exert a disproportionate influence on derived mean values. To address this, all measurements in the data set were assigned
16 to 1° spatial bins, in which all observations for a given year were averaged. [All observations within the JJA months for a given](#)
17 [year were averaged, rather than deriving separate monthly climatologies](#). The resulting yearly data grids were then averaged
18 to create long-term gridded means. This technique effectively assigns equal weight to each year of measurements in a given
19 grid cell. Both DMS and paired ancillary parameters were binned using this method.
20

21 Following the approach of L11, data grid cells were assigned to Longhurst Biogeochemical Provinces to examine patterns
22 across different regimes within the greater NESAP (Longhurst 2007). Three primary provinces fall within the domain of our
23 study region: California Upwelling Coastal Province (CCAL), Alaska Downwelling Coastal Province (ALSK), and Pacific
24 Subarctic Gyres Province – East (PSAE) (Fig. 8). The CCAL province as defined by Longhurst extends south to 16.5° N.
25 Hereafter, all references to the CCAL refer to the portion of this province above 44.5° N latitude. Province boundary
26 designations were obtained from www.marineregions.com (accessed October 2017), and the MATLAB native inpolygon.m
27 function was used to assign grid cells to individual provinces. Any grid cell either inside or on the edge of boundaries was
28 assigned to a particular province. As such, some data cells (37 out of 249 total) are assigned to multiple provinces. Average
29 summer DMS concentrations and flux measurements were computed for each province. For comparison to L11, we
30 recalculated the average summertime DMS concentration and flux in the three study provinces using only the PMEL data
31 utilized by L11. [The PMEL data](#) were first binned using the year-weighted method described above.

1 2.6 Statistical analysis and empirical algorithms

2 We used our compiled data set to examine broad-scale relationships between DMS and other oceanographic variables. For
3 this analysis, data were log-transformed to overcome non-normal distributions, and the strength of pair-wise relationships was
4 assessed by computing Pearson's correlation coefficients. Correlations were applied to $1^\circ \times 1^\circ$ binned data both within
5 individual provinces and across the entire NESAP.

6
7 We also used several existing empirical algorithms to reconstruct DMS fields at a $1^\circ \times 1^\circ$ resolution from various environmental
8 predictor variables, comparing the accuracy of the resultant products against our binned DMS observations. The algorithms
9 tested in this study include those of Simó and Dachs (2002), Vallina and Simó (2007), Watanabe et al. (2007), and Galí et al.
10 (2018) (hereafter, SD02, VS07, W07, and G18, respectively). Both SD02 and VS07 used global data bases to develop their
11 algorithms. SD02 relates DMS to chl-*a*:MLD, with chl-*a* values $> 15 \mu\text{g L}^{-1}$ removed prior to analysis. VS07 relates DMS
12 concentration to solar radiative dose (SRD). This term, as defined by the authors, is based on light extinction coefficients (k_d),
13 sea surface irradiance (I_0), and mixed layer depth. Due to the large areal extent of the study area, we used AquaMODIS derived
14 PAR in lieu of the station-based I_0 measurements used by the authors. Similarly, strong variation in k_d in coastal vs. open
15 ocean waters is expected. We thus modified the author's approach and used satellite derived k_d (based on a chlorophyll-
16 dependent algorithm; Werdell and Bailey 2005) rather than a fixed coefficient. W07 uses data specific to the North Pacific
17 and relates DMS to SST, SSN and latitude. [The two-step G18 algorithm utilizes a previously developed DMSpt predictive](#)
18 [algorithm based on chl-*a* and MLD \(Galí et al. 2015\), in conjunction with PAR measurements. In order to test this algorithm,](#)
19 [we utilized the satellite-derived PAR, MLD and chl-*a*, described above. We further modify the author's approach by testing](#)
20 [performance on our \$1^\circ \times 1^\circ\$ binned data, rather than data binned at a \$5^\circ \times 5^\circ\$, in order to maximize the number of observations.](#)
21 Recognizing the utility of re-parameterizing proposed algorithms for specific areas, we tested algorithms using both published
22 linear coefficients, and coefficients derived specifically for the NESAP using a least-squares approach to determine best fit to
23 our data set. [The coefficients used to test the original G18 were those regionally tuned by the authors for latitudes above \$45^\circ\$](#)
24 [N.](#)

25 3 Results

26 We begin by presenting an overview of our new DMS measurements and ancillary data from the 2016–2017 summer cruises,
27 highlighting DMS distributions and the presence of distinct surface water properties across different parts of our transect. We
28 then provide a detailed description of DMS dynamics across several hydrographic frontal zones, discussing the potential role
29 of various processes in driving these gradients. Finally, we [present](#) an updated summertime climatology for this region,
30 compiling our new measurements with existing DMS observations from across the NESAP to examine large-scale patterns in
31 DMS distributions, and correlations with other oceanographic variables. The potential role of these variables in driving DMS
32 distributions in the NESAP, and the need for additional process studies is addressed in the discussion.

1 **3.1 Oceanographic conditions in the NESAP during summer 2016–2017**

2 Our 2016 and 2017 cruises surveyed oceanographic regimes from offshore HNLC regions to productive coastal upwelling
3 zones. As indicated by AquaMODIS satellite imagery, chl-*a* concentrations exhibited strong gradients across the oceanic-
4 coastal transition in both 2016 and 2017 (Fig. 1). Coastal waters showed elevated chl-*a*, with maximum values of 50 $\mu\text{g L}^{-1}$
5 and 18 $\mu\text{g L}^{-1}$ in 2016 and 2017, respectively. In both years, highest chl-*a* values were observed in waters with shallow mixed-
6 layer depths (<10 m) along the La Perouse Bank (Fig. 1). In the off-shelf regions, chl-*a* concentrations appeared uniformly
7 low in 2016, although significant cloud cover limited the availability of satellite imagery. By comparison, we observed
8 generally higher chl-*a* concentrations in offshore waters in 2017. Most notably, our cruise track passed through an apparent
9 coccolithophore bloom in the northern Gulf of Alaska, where a large calcite signal ($\sim 2 \text{ mmol PIC m}^{-3}$) was detected in
10 AquaMODIS imagery. Patterns in NCP were generally similar to those of chl-*a*, with elevated production in coastal waters
11 (Fig. 2c). In both years, we observed NCP on La Perouse Bank exceeding 100 $\text{mmol O}_2 \text{ m}^{-2} \text{ d}^{-1}$ (Fig. 2c, inset).

12
13 Coastal regions exhibited generally fresher surface waters and shallower mixed layer depths, except for several regions of
14 enhanced vertical mixing associated with upwelling. This coastal upwelling signature was apparent in elevated salinity and
15 decreased temperature of surface waters, and also through the presence of negative sea surface height anomalies (Fig. 1c,d).
16 Small-scale regional heterogeneity in coastal regions was apparent in both years, with salinity and temperature exhibiting sharp
17 gradients over the continental shelf, associated with riverine input and complex mixing processes. By comparison, oceanic
18 surface waters showed less spatial heterogeneity, and were generally more saline, with deeper mixed layers (Fig. 2b). The
19 sea-surface height anomaly field indicated the presence of several Sitka and Haida eddies in both years (Fig. 1c,d), enhancing
20 mesoscale variability through the transport of coastal water offshore.

21
22 Using the approach of Hirata et al. (2011) and Zeng et al. (2018), we derived high resolution estimates of phytoplankton
23 assemblage composition from our underway chl-*a* measurements. This approach revealed a predominance of phytoplankton
24 in the micro- size class ($>20 \mu\text{m}$) in coastal waters (Fig. 2d), with an average of 50 % of chl-*a* attributable to
25 microphytoplankton. In contrast, off-shelf waters showed greater diversity in phytoplankton composition. In these waters,
26 microphytoplankton accounted for ~ 25 % of total chl-*a*, while the pico- and nano- size classes accounted for ~ 30 % and ~ 40
27 %, respectively (Fig. 2e,f).

28 **3.2 DMS distributions**

29 Across our study region, surface water DMS concentrations ranged from $<1\text{--}24 \text{ nM}$ in 2016 and $<1\text{--}18 \text{ nM}$ in 2017 (Fig. 2a,
30 Fig. 3). We observed a number of localized DMS ‘hot spots’ in regions of elevated chl-*a* and NCP. In both years, these
31 localized high DMS regions were particularly evident in the vicinity of the highly productive La Perouse Bank (Fig. 2a, inset).
32 We also observed several areas where strong DMS gradients co-occurred with salinity fronts. These areas include the T1–T3
33 transects survey in O16, detailed below. Despite associations between DMS concentration and several variables in some

1 localized regions, we only observed weak correlations between DMS and other measured variables across the full cruise tracks.
2 During O16, DMS concentrations were most strongly correlated to NCP, with a Pearson's coefficient of $r=0.42$ ($p<0.001$).
3 This relationship was substantially weaker in O17 ($r=0.29$, $p<0.001$).

4 **3.3 Detailed surveys of DMS across hydrographic frontal zones**

5 During the O16 cruise, we sampled along three repeated transects to map DMS distributions near hydrographic frontal zones.
6 All three transects showed significant gradients in salinity, chl-*a* and DMS/P concentrations, as well as in the metabolic activity
7 of phytoplankton and bacteria (Fig. 4, 6–7). While DMS concentrations appeared to co-vary with salinity and chl-*a* across
8 these frontal zones, the strength and direction of these relationships were not consistent across the three transects. We discuss
9 each transect in detail below.

10 **3.3.1 Transect 1**

11 T1 was located west of Dixon Entrance (Fig. 1) in waters influenced by the Alaska Current and coastal water masses. Offshore
12 waters along this transect were more saline and colder than those on the shelf. The area exhibited DMS concentrations up to
13 10 nM in off-shelf, saline waters (Fig. 4). [Particulate and dissolved DMSP ranged from ~60–125 nM and ~1.8–4.7 nM,](#)
14 [respectively, and showed no significant correlation to DMS \(Fig. 4d\).](#) At the shelf break (approx. 134.4° W, indicated on Fig.
15 4 by dotted line), we measured a sharp drop in salinity and corresponding decrease in DMS concentrations, with concentrations
16 remaining below ~3 nM over the most coastal parts of the transect. Across the entire T1 transect, DMS concentrations
17 displayed a striking fine-scale coherence to salinity ($r=0.80$, $p<0.001$; Fig. 4a,b). A significant positive correlation was also
18 observed with SSHA ($r=0.51$, $p<0.001$), indicating a potential influence of westward-propagating Haida eddies. Fig. 5 shows
19 a line plot of SSHA measurements from the approximate time of T1 sampling, overlaid by DMS concentrations. [The coherence](#)
20 [between DMS concentrations and mesoscale oceanographic features can be seen in this figure despite differences in the spatial](#)
21 [resolution of the two data sets.](#)

22
23 The lower salinity coastal waters [along T1](#) were characterized by elevated chl-*a* concentrations (Fig. 4c), resulting in a negative
24 correlation between DMS concentrations and chlorophyll ($r=-0.47$, $p<0.001$). Figure 4c shows the estimated percent
25 abundance of [diatoms and combined dinoflagellates and prymnesiophytes](#) as derived from HPLC-based DPA-analysis. [The](#)
26 [remaining phytoplankton assemblage consisted largely of picoeukaryotes \(13 – 36 %\).](#) Although HPLC samples are not
27 available for all of the coastal waters we sampled, results obtained from the empirical algorithm of Hirata et al. (2011) [using](#)
28 [underway absorption data](#) suggest a shift in phytoplankton assemblage composition [from](#) smaller size classes in offshore waters
29 to a microphytoplankton-dominated community in on-shelf waters. DMS exhibited relatively weak, though statistically
30 significant ($p<0.001$) positive correlations with the [algorithm-derived relative](#) abundance of nano- and picophytoplankton size-
31 classes ($r=0.55$ and $r=0.38$, respectively), and a negative correlation with the relative abundance of microphytoplankton ($r=-$
32 0.53). In support of this result, [discrete](#) HPLC measurements revealed a strong positive relationship between DMS
33 concentration and [the combined](#) relative abundance of prymnesiophytes [and dinoflagellates](#) ($r=0.89$, $p=0.001$), and a negative

1 correlation to diatom abundance ($r=-0.70$, $p=0.036$). We also observed a strong positive correlation between DMS and
2 DMSP_{p:chl-a} ($r=0.80$, $p=0.003$) suggesting higher cellular DMSP concentrations in phytoplankton assemblages in the off-
3 shelf regions of this transect. Overall, results from this transect demonstrate a transition from high DMS concentrations in the
4 lower productivity, nano-phytoplankton dominated offshore waters, to low DMS concentrations in higher productivity, diatom-
5 dominated nearshore region.

6
7 Average rate constants (d^{-1}) for biological consumption of DMS and DMSP_d appeared qualitatively higher in the on-shelf
8 region (although insufficient sampling does not allow for reliable statistical testing), suggesting faster removal of DMS/P from
9 coastal surface waters with lower DMS concentrations. For DMS and DMSP_d respectively, loss constants averaged $1.15 \pm$
10 $0.3 d^{-1}$ and $88.2 \pm 13.9 d^{-1}$ onshore, as compared to $0.66 \pm 0.045 d^{-1}$ and $39.6 \pm 1.45 d^{-1}$ in offshore stations (Fig. 4e). Net
11 primary productivity and bacterial productivity also showed a qualitative trend towards higher average values in the low DMS
12 coastal waters, but these differences were not statistically significant. Although biological loss of DMS constitutes only one
13 of several loss terms, the patterns observed here suggest that enhanced microbial activity and relatively higher DMS/P
14 consumption rate constants played a role in maintaining lower concentrations of these compounds in nearshore waters.

15
16 We calculated the mixed layer DMS burden by multiplying concentration and average mixed layer depth (13 m). Biological
17 DMS loss integrated over the mixed layer averaged $22 \mu\text{mol m}^{-2} d^{-1}$, sufficient for daily removal of 47 % of the DMS burden.
18 By comparison, derived sea-air flux estimates across the transect exhibited a mean value of $13 \mu\text{mol DMS m}^{-2} d^{-1}$, accounting
19 for ~ 25 % of the mixed layer DMS burden daily. Due to a relatively homogenous wind field over the area of our sampling
20 transect, the sea-air fluxes were tightly correlated to DMS concentrations, such that the lower DMS concentrations in nearshore
21 regions cannot be explained by greater rates of ventilation to the atmosphere.

22 3.3.2 Transect 2

23 The second sampling transect, T2, was located in the coastal waters of Hecate Strait situated on the continental shelf (Fig. 1).
24 Sea surface temperatures along this transect exhibited low variability (standard deviation $\sim 0.5^\circ \text{C}$), with the coldest waters
25 located mid-transect in areas of highest chl-*a*. Mixed layer depths ranged from 10–15 m, and DMS concentrations ranged
26 from $< 0.5 \text{ nM}$ to nearly 20 nM (Fig. 6). DMSP_d concentrations exhibited only minor variations over the transect (2.5–2.8
27 nM), while DMSP_p concentrations showed greater variability (61–144 nM). Neither
28 DMSP_d or DMSP_p were correlated to DMS concentrations. HPLC measurements suggested that diatoms dominated across
29 the entire transect, and particularly in northern regions (Fig. 6c). Picoeukaryotes and green algae comprised the bulk of the
30 remaining phytoplankton assemblage composition (generally $< 10 \%$). In contrast to our observations for T1, DMS
31 concentrations exhibited negative correlations to both salinity ($r=-0.69$, $p<0.001$; Fig. 6b) and SSHA ($r=-0.81$, $p<0.001$) in this
32 area and were not significantly correlated to chl-*a* (Fig. 6c). Despite the lack of correlation to chl-*a*, DMS did exhibit
33 significant, though weak, positive correlations with estimates of relative microphytoplankton abundance ($r=0.22$, $p<0.001$),
34 and stronger negative correlations with the abundance of pico- and nano- size classes (T2: $r=-0.47$, $r=-0.45$; $p<0.001$; Fig. 6c).

1 In support of this observation, HPLC-pigment data from discrete sampling stations revealed a strong positive relationship
2 between DMS concentration and relative abundance of diatoms ($r=0.88$, $p=0.001$), and a negative correlation between DMS
3 and combined dinoflagellate and prymnesiophyte abundance ($r=-0.88$, $p=0.001$). These correlations suggest diatoms as an
4 important source of DMS, in contrast to that observed for T1.

5
6 Unlike bulk chl-*a* concentrations, we found that primary productivity showed a strong positive correlation with DMS along
7 T2 ($r=0.90$, $p=0.037$), although this result is based on only four data points. Bacterial productivity was also significantly higher
8 in the high DMS waters, although this variable was even more sparsely sampled along the transect, and we cannot infer any
9 meaningful statistical association with DMS (Fig. 6f). As with T1, both k_{DMSPd} and k_{DMS} appeared higher in the low-DMS
10 portions of the transect. Across the entire transect, DMS and DMSP consumption rate constants ranged from 0.51 to 1.29 d⁻¹
11 and 28.8 to 49.5 d⁻¹, respectively (Fig. 6e). This result suggests microbial consumption as potential driver of DMS
12 distributions, with higher DMS/P consumption rate constants in waters with lower DMS concentrations.

13
14 Integrated biological DMS loss was significantly higher than that of T1, with an average 78 $\mu\text{mol m}^{-2} \text{d}^{-1}$ (equivalent to removal
15 of 87 % of the DMS burden per day). By comparison, DMS sea-air flux across the transect was low, with a mean value of 2.9
16 $\mu\text{mol m}^{-2} \text{d}^{-1}$. This flux was sufficient to remove only ~6 % of mixed layer DMS burden daily. We thus conclude that biological
17 processes play a significant role in DMS turn-over along this transect.

18 3.3.3 Transect 3

19 T3 was located in the highly productive coastal waters of La Perouse Bank, along the continental shelf of the west coast of
20 Vancouver Island (Fig. 1). DMS concentrations across this transect ranged from <1–24 nM, while DMSPd and DMSPp
21 concentrations were among the highest observed cruise-wide (1.1 – 9.8 nM and 26 – 480 nM, respectively; Fig. 7d). DMSPp
22 was correlated to DMS ($r=0.76$, $p=0.02$). Mixed layer depths ranged from 8–12 m, with the shallowest values found in fresher,
23 salinity-stratified inshore waters influenced by riverine input. Sea surface temperature was lower in these low salinity waters,
24 although it varied little over the transect (standard deviation < 1 °C). With respect to other measured variables, DMS behaved
25 similarly to the coastal T2 transect (Fig. 7a). We observed negative correlations between DMS and salinity ($r=-0.78$, $p<0.001$;
26 Fig. 7b) and SSHA ($r=-0.75$, $p<0.001$). We also found elevated chl-*a* in the low salinity waters, although there was only a
27 weak positive correlation between chl-*a* and DMS ($r=0.25$, $p<0.001$) across the full transect (Fig. 7c).

28
29 Microphytoplankton consisting primarily of diatoms dominated the low-salinity, high-DMS waters of the transect, with a shift
30 towards smaller cells observed in the more saline waters farther offshore (Fig. 7c). Among the T3 stations, green algae,
31 prokaryotes, and picoeukaryotes each comprised ~5 – 20 % of phytoplankton abundance. Similar to T2, we found a significant
32 positive correlation between DMS and microphytoplankton ($r=0.90$, $p<0.001$), and a negative correlation between DMS and
33 phytoplankton of the nano- and pico- size class ($r=-0.77$, $r=-0.75$; $p<0.001$). In support of this observation, HPLC-pigment
34 data showed a strong positive relationship between DMS concentration and relative abundance of diatoms ($r=0.94$, $p<0.001$),

1 and a negative correlation with [combined dinoflagellate and prymnesiophyte abundance](#) ($r=-0.74$, $p=0.023$). A negative
2 relationship was also observed between DMSP:chl-*a* and DMS ($r=-0.88$, $p=0.002$) (Fig. 7d). In contrast to T1, high DMS
3 coincided with regions of lower cellular DMSP concentrations among phytoplankton, consistent with the dominance of
4 diatoms in the high DMS portions of this transect.

5
6 Along the T3 transect, DMS [exhibited](#) a positive [qualitative](#) association with primary productivity and bacterial productivity,
7 though these relationships are based on very few sampling points. It is noteworthy that the bacterial productivity measured
8 along T3 was higher than anywhere else along the cruise track, with production more than 5-fold greater than the cruise-wide
9 average. Values of k_{DMS} ranged from 0.8–2.7 d^{-1} across the transect. As with T1 and T2, k_{DMS} was higher in low-DMS regions
10 of T3. In contrast, k_{DMSPd} values along T3 increased in parallel with DMS concentrations (higher rate constants in higher DMS
11 waters). DMSP loss constants ranged from 38.6 to 92.1 d^{-1} (Fig. 7e). The highest DMSP loss constant translates into a derived
12 turnover time of just 16 minutes, [and coincided with the highest bacterial productivity \(~26 \$\mu g\$ POC \$L^{-1} d^{-1}\$ \)](#).

13
14 Biological DMS loss integrated over the mixed layer was sufficiently high to remove >100 % of the DMS burden daily (~47
15 $\mu mol m^{-2} d^{-1}$). [By comparison](#), sea–air fluxes were a minor loss term by comparison (4.9 $\mu mol m^{-2} d^{-1}$), and were sufficient to
16 remove only ~12 % of the mixed layer DMS burden. Due to low removal rates and relative homogeneity of wind speed fields,
17 sea–air flux cannot be invoked to explain the spatial distribution of DMS across this transect.

18 **3.4 Regional DMS distribution – comparisons of 2016 and 2017 observations with past studies**

19 To explore potential regional-scale relationships between DMS concentrations and other environmental variables, we
20 combined our new DMS data with measurements collected over the past three decades, including previously unpublished high-
21 resolution MIMS data. The addition of new measurements to the existing PMEL data set substantially increases spatial and
22 temporal coverage in the NESAP. When data were binned to $1^\circ \times 1^\circ$ resolution, coverage was increased by ~20 % in the
23 CCAL and ALSK Longhurst provinces, and 14 % in the PSAE, with the overall addition of 90 data-containing grid cells (Table
24 2). As shown in Fig. 8, our measurements primarily increase data coverage in waters below $57^\circ N$. These regions were
25 previously under-sampled in the PMEL data set utilized by L11, which was strongly biased to measurements near the coast of
26 Alaska. Figure 9a further illustrates the latitudinal shift in data coverage with the inclusion of additional MIMS data. As
27 shown in Fig. 9b, average derived DMS concentrations across latitudinal bands at the north and south extremes of our study
28 area remain similar to those derived from the PMEL data set utilized by L11. However, in the region between $50^\circ N$ and 54°
29 N , where there were few observations in the PMEL database, our compiled data show mean concentrations as much as 4.5 nM
30 (~40 %) lower than those calculated using PMEL data alone.

31
32 Table 3 shows the change in province-wide average DMS concentration, sea–air fluxes, and total summertime DMS flux based
33 on our updated analysis. Relative to our revised estimates, DMS concentrations and [sea-air fluxes](#) derived using only the
34 PMEL data were lower in the CCAL and higher in both the PSAE and ALSK provinces. The most pronounced difference was

1 that of sea–air flux in the PSAE, where estimated [values](#) decreased by $4.5 \mu\text{mol m}^{-2} \text{d}^{-1}$ (20 %). Despite these regional
2 differences, the total summer DMS flux across the NESAP differed by only 6.5 % between our compiled data set (0.30 Tg S)
3 and the PMEL data set utilized by L11 (0.32 Tg S).

4
5 Our compiled data set provides greater confidence in DMS concentrations and sea–air fluxes across the NESAP, and enables
6 us to better constrain spatial patterns. Figure 10 shows binned average summertime DMS concentration across the region, as
7 well as the derived sea–air DMS fluxes. The highest concentrations [were](#) observed in ALSK, where coastal waters contain
8 maximum DMS concentrations exceeding 20 nM. A persistent region of elevated DMS concentrations [was](#) also evident in
9 mid-PSAE oceanic region, with concentrations greater than 10 nM. Sea–air DMS fluxes [showed](#) a spatial distribution [similar](#)
10 [to](#) DMS concentrations, with maximum values of $>100 \mu\text{mol m}^{-2} \text{d}^{-1}$. [Calculated DMS:chl-*a* ratios](#) for binned data (Fig. 10c),
11 [showed](#) generally higher [values](#) in offshore NESAP waters.

12 **3.5 Correlations and algorithm testing**

13 Using our new data compilation, we examined the relationship between DMS concentrations and a suite of oceanographic
14 variables across the NESAP. Table 4 shows both NESAP-wide and province-specific correlations derived from this analysis.
15 While many correlations are weak or not statistically significant, some patterns do emerge, particularly in the offshore waters
16 of the PSAE domain. No single variable explains a large portion of the DMS variation in this province, but statistically
17 significant correlations exist between DMS and chl-*a* and calcite ($r=0.45$ and $r=0.50$, respectively). We also found a negative
18 relationship between DMS and SSHA ($r=-0.47$). For the ALSK province, we found weak inverse correlations between DMS
19 and SST ($r=-0.32$) and water depth ($r=-0.34$). Significant positive correlations between DMS and derived surface NO_3
20 concentrations, PAR, and chl-*a* are also observed ($r=0.30$, $r=0.41$, and $r=0.34$ respectively). In contrast to other provinces, we
21 observed a statistically significant correlation between DMS and NCP in the CCAL province ($r=0.43$). The lack of other
22 significant correlations in the province may, in part, reflect the lower number of data points obtained for this region.

23
24 Moving beyond simple pairwise correlations, multi-variate empirical algorithms provide an additional approach to assess the
25 potential drivers of regional DMS dynamics. We evaluated the ability of [five](#) previously published algorithms to reproduce
26 patterns in the DMS observations. In order to obtain the best possible results, we modified the original equations [using](#) a least
27 squares method to obtain the best-fit coefficients for our data set. We evaluated the algorithm outputs against observations
28 using Pearson’s correlation coefficients and root mean square errors (RMSE). As shown in Table 5, model performance was
29 generally low, with [most](#) correlation coefficients less than [0.53](#) and RMSE values ranging from 1.2 to 81.6 nM. [The best](#)
30 [results were obtained for the CCAL province, where both the tuned SD02 and the original G18 algorithms were able to predict](#)
31 [DMS concentrations with moderate success \(\$r = 0.62^*\$, RMSE = 1.61 and \$r = 0.72^*\$, RMSE = 1.9, for SD02 and G18,](#)
32 [respectively\). As both of these algorithms rely on MLD, which is only available for waters deeper than 2000 m, it is important](#)
33 [to note that predictive strength can only be assessed for these off-shelf waters, and should not be taken to represent performance](#)
34 [in coastal waters.](#) The customized VS07 (with coefficients tuned to the NESAP data) showed the best overall performance

1 across the entire NESAP region. Yet, even this model showed only weak correlation between predicted and observed DMS
2 values ($r=0.31$). [Notably](#), the original linear coefficients for this model yielded DMS concentrations that were inversely
3 correlated to the measured values. In no case did models using original linear coefficients outperform those using recalculated
4 coefficients.

5 **4 Discussion**

6 [The results presented here](#) provide new information on the fine-scale and regional patterns of DMS distributions across the
7 NESAP. Our ship-board observations document sub-mesoscale variability in DMS concentration across hydrographic frontal
8 zones, with associated process measurements providing insight into potential driving factors. By combining these new data
9 with more than three decades of DMS measurements, we are able to improve data coverage for the NESAP to examine larger-
10 scale spatial patterns and provide a more robust regional climatology to evaluate empirical predictive algorithms.

11 **4.1 Contrasting cycling regimes within the NESAP**

12 A number of studies have documented differences in DMS dynamics across oceanographic regimes in the NESAP (Royer et
13 al. 2010, Asher et al. 2011, 2017). These regional differences result from complex ecosystem and environmental interactions,
14 and limit broad-scale prediction of DMS concentrations and sea–air fluxes (Galí et al. 2018). Taxonomic composition of
15 phytoplankton assemblages has been identified as a main driver of DMS distribution patterns. For example, dinoflagellates
16 and prymnesiophytes typically have elevated DMS production, associated with greater intracellular concentrations of DMSP
17 [\(Keller 1989\)](#) and, in some cases, high activity of DMSP lyase (the enzyme that cleaves DMSP to DMS and acrylate; Steinke
18 et al. 2002; Wolfe et al. 2002; Curson et al. 2018). In contrast, bloom-forming diatom species have typically lower intracellular
19 DMSP levels [\(Keller 1989\)](#), [with the exception of some polar species \(Levasseur et al. 1994, Matrai and Vernet 1997\)](#).
20 However, nutrient limitation has been shown to significantly increase diatom DMS/P production [\(Bucciarelli and Sunda 2003;](#)
21 [Sunda et al. 2007; Harada et al. 2009\)](#). Thus, the accumulation of DMS in the water column depends on both the composition
22 of phytoplankton assemblages and their physiological state, [as previously shown by Gabric et al. \(1999\)](#). Other factors,
23 including zooplankton grazing and the metabolic demands of heterotrophic bacteria are also important [\(e.g. Levasseur et al.](#)
24 [1996, Kiene and Linn 2000, Merzouk et al. 2006, Asher et al. 2017\)](#). Below, we discuss the potential factors driving high
25 DMS concentrations along three frontal zones exhibiting sharp DMS concentration gradients. Specifically, we contrast the
26 nanoplankton dominated T1 transect with the diatom-dominated coastal T2 and T3 transects, examining the environmental
27 and biological conditions that may have led to the different DMS accumulation in these areas.

28 **4.2 The importance of phytoplankton assemblage composition**

29 The T1 transect, located in the southern-most portion of the ALSK province, spanned 5° of longitude from deep (>3000 m)
30 offshore waters, into nearshore waters over the continental shelf. These oceanographic regimes were separated by strong
31 hydrographic frontal features in the vicinity of the shelf break. The negative correlation between DMS and chl-*a* along this

1 transect demonstrates that DMS accumulation did not directly scale with bulk phytoplankton biomass. Rather, our results
2 suggest that DMS concentrations were likely influenced by phytoplankton assemblage composition, with the highest DMS
3 concentrations associated with the greatest relative proportion of prymnesiophytes [and dinoflagellates](#) (Fig. 4c) and the highest
4 DMSP_p:chl-*a* (Fig. 4d). Similar relationships have been documented in numerous studies focusing on offshore waters of the
5 NESAP [and elsewhere](#) (e.g. [Barnard et al. 1984](#); [Hatton et al. 1999](#); [Royer et al. 2010](#); [Steiner et al. 2012](#)). In these areas,
6 elevated DMS concentrations are often attributed to a preponderance of high-DMSP phytoplankton taxa.

7

8 Comparison of T2 and T3 with T1 shows that the association of elevated DMS with prymnesiophyte [and dinoflagellate](#)
9 dominance and high DMSP_p:chl-*a* ratios did not hold across our entire survey region. As was observed [by Royer et al. \(2010\)](#),
10 we measured generally low DMSP_p:chl-*a* ratios in the diatom-dominated coastal waters of T2 and T3 (Fig. 6d, 7d). Yet, DMS
11 concentrations measured in these waters were extremely high, at times exceeding 20 nM (Fig. 2a). Unlike the T1 transect,
12 DMS concentrations along T2 and T3 increased with decreasing DMSP_p:chl-*a* ratios, and were strongly correlated with diatom
13 abundance.

14

15 One potential explanation for the difference between T1 and T2/T3 may relate to the different location of these sampling
16 regions. The T1 transect sits along the transition between offshore and inshore waters, where different nutrient regimes control
17 phytoplankton productivity. Inshore waters over the continental shelf are typically limited by macronutrients, whereas offshore
18 waters transition into iron-limitation (Boyd and Harrison 1999). At the boundary between these regimes, mixing of water
19 masses through horizontal advection can stimulate phytoplankton productivity (Lam and Letters 2008). Ribalet et al. (2010)
20 observed an active community of nanoplankton in the transitional waters, and attributed this to the stimulation of (often high-
21 DMSP) oceanic phytoplankton by water mass mixing, at the boundary of macro- and micro-nutrient rich waters.

22 [Formation of Haida and Sitka eddies may aid in this mixing through the westward transportation of micronutrient-replete](#)
23 [coastal water](#) (Johnson et al. 2005; Whitney et al. 2005). [SSHA measurements can be used as an indicator of eddy-induced](#)
24 [mixing in this region, as warm-core Haida and Sitka eddies waters manifest as closed circulation features exhibiting positive](#)
25 [SSHA \(Fig. 1c, d\)](#). We observed the highest DMS associated with positive SSHA along T1 (Fig. 5), [suggesting the influence](#)
26 [of water mass mixing in driving mesoscale patterns of DMS distribution. Beyond this mesoscale coherence, unresolved sub-](#)
27 [mesoscale variability is likely attributable to biological heterogeneity \(Fig. 4c, d; Royer 2015 et al.\)](#)

28

29 In contrast to the transition waters, nearshore waters over the continental shelf are typically dominated by low DMSP-
30 producing diatoms. Elevated DMS in these diatom-rich waters may reflect a combination of high absolute biomass and an
31 upregulation of DMSP production observed under nutrient stress (Bucciarelli and Sunda 2003; Sunda et al. 2007; Hockin et
32 al. 2012; Bucciarelli et al. 2013). A meta-analysis by McParland and Levine ([2018](#)) reported an average 12-fold upregulation
33 of intracellular DMSP production under nutrient-stress conditions among phytoplankton, [including diatoms](#), typically
34 considered low-producers. By comparison, high DMSP producers only showed an average 1.4-fold upregulation. [Our results](#)
35 [are similar to those of Barnard et al. \(1984\), who observed a decreasing influence of prymnesiophyte abundance on DMS](#)

1 [concentrations in the Bering Sea with increasing proximity to the continental shelf. We note that increases in](#)
2 [microphytoplankton abundances are often accompanied by increases in other phytoplankton groups \(including high-DMSP](#)
3 [producing taxa; Barber and Hiscock 2006; Uitz et al. 2006\). However, we observed no correlation between DMS and the](#)
4 [absolute abundance of prymnesiophytes and dinoflagellates for either T2 or T3 transects. This result suggests that while these](#)
5 [high-DMSP producing taxa may play a role in driving DMS concentrations along these transect, diatoms are likely dominant](#)
6 [contributors, as judged by the strong correlation between DMS and absolute diatom absolute abundance \(\$r=0.91\$, \$p=0.001\$ \)](#)
7 [along T3.](#)

8
9 In coastal waters, seasonal upwelling may drive high phytoplankton biomass accumulation and increased DMS production in
10 the late-bloom phase, when stratified surface layers are exposed to higher mean light intensities (due to shallow mixing) and
11 become nutrient [depleted](#) (Zindler et al. 2012). These environmental conditions would act to increase cellular oxidative stress,
12 thus promoting the production of DMS/P as part of a [cellular](#) response mechanism (Sunda et al. 2002). [Further, several studies](#)
13 [have shown increased bacterial activity and higher rates of cellular DMSP leakage in the late-bloom phase \(Malin et al. 1993;](#)
14 [Stefels and Boeckel 1993; Matrai and Keller 1994\).](#) The results of Asher et al. (2017) demonstrating high DMS concentrations
15 in post-upwelling waters [of the coastal NESAP](#) support this idea. Measurements of SSHA in coastal regions can provide a
16 signature for recent upwelling; [the combined effect of wind-induced seasonal water transport offshore and the presence of high](#)
17 [density \(cold and saline\) upwelled water acts to depress sea surface height relative to annual means \(Smith 1974; Tabata et al.](#)
18 [1986; Strub and James 1995; Saraceno et al. 2008; Venegas et al. 2008\).](#) Negative relationships between DMS concentrations
19 and SSHA were observed in both the T2 and T3 transects, suggesting an association between DMS and upwelling events.

20
21 Additional ecosystem processes may influence DMS accumulation in surface waters. In particular, zooplankton grazing and
22 viral infection may increase DMS concentrations, due to the release of cellular DMSP in phytoplankton during sloppy feeding
23 and cellular lysis ([Dacey and Wakeham 1986; Belviso et al. 1990; Hill et al. 1998](#)). Both of these factors are density-dependent,
24 and thus likely to become more significant with higher phytoplankton cell densities in the late bloom phase. Unfortunately,
25 we do not have measurements to address these processes directly, but the elevated DMSPd concentrations along T3 (~7 nM)
26 may reflect viral and zooplankton mediated loss of particulate DMSP into the dissolved pool.

27
28 Taken together, our results support previous studies showing the importance of DMSP-rich species in driving high DMS
29 concentration in offshore waters of the NESAP [and elsewhere \(e.g Stefels et al. 2007, Royer et al. 2010, Steiner et al. 2012,](#)
30 [Asher et al. 2017\)](#). In coastal waters, it appears that diatom-dominated phytoplankton assemblages can also support elevated
31 DMS accumulation, particularly under high biomass conditions during the late bloom phase, [as has been previously observed](#)
32 [in the Southern Ocean \(Turner et al. 1995\) and the Barents Sea \(Matrai and Vernet 1997\).](#)

1 4.3 The effect of DMS/P consumption rate on DMS distribution

2 DMS consumption rates constants across our study area can be translated to biological DMS turnover times ranging from 9 h
3 to 2.5 d (average of 25 h). By comparison, turnover times calculated from sea–air flux removal rates averaged 6.1 d across
4 this area, suggesting that this term is less important in the mixed layer DMS budget. We note that DMS concentration is set
5 by the dynamic balance between production and loss terms (Galí and Simó, 2015), of which only a subset were measured in
6 our study. Gross DMS production, DMS production from DMSP cleavage, and DMS loss from photo-oxidation, which we
7 did not measure, constitute potentially important terms in driving DMS distribution. Further, our conclusions are limited by
8 data coverage, and based, at times, on few measurements. Notwithstanding these limitations, to our knowledge, no study has
9 yet assessed DMS/P turnover rates across frontal zones on the small spatial scales examined here. Our limited measurements
10 thus remain important in comparing meso- and submesoscale processes to those operating on larger spatial scales. While these
11 measures do not encompass all loss processes, we found that biological consumption and sea–air flux alone were sufficient to
12 quickly erase a DMS accumulation signature in the mixed layer. Thus, DMS concentrations measured here appear to be
13 reflective of short-term production and consumption processes.

14
15 Across our study area, biological DMS removal rate constants (d^{-1}) were inversely related to DMS concentrations ($r=-0.55$,
16 $p=0.03$), with lower k_{DMS} in waters with elevated DMS. This study-wide trend supports the relationships observed along each
17 transect. The relationship may reflect a time-lag of bacterial response to increased DMS concentrations. Results from previous
18 studies in other regions have shown that bacterial DMS consumption increases after a rapid rise in DMS concentrations,
19 resulting in consumption rate constants that are relatively low when DMS concentrations are initially high. As consumption
20 rate constants increase, DMS concentrations decrease (Zubkov et al. 2004; del Valle et al. 2009). These results, along with
21 the observed positive correlation between DMS and bacterial activity ($r=0.53$, $p=0.03$), suggest that microbial consumption is
22 an important control on DMS accumulation, irrespective of phytoplankton community assemblage. However, the positive
23 correlation between DMS loss rates and concentrations suggests that microbial consumption may not be sufficient to offset
24 new DMS production. Previous studies in other regions have examined the impact of DMS loss and production in driving
25 distributions, demonstrating correlations between DMS concentrations and microbial consumption and production rates in
26 some systems (Wolfe and Kiene 1993; Zubkov et al. 2002 Merzouk et al. 2006, Vila-Costa et al. 2008). The relationship
27 observed here between DMS , k_{DMS} and bacterial activity may reflect the preponderance of on-shelf stations measured for DMS
28 consumption in our survey (10 out of 16 stations), and significantly higher rates of bacterial metabolism in onshore waters
29 (7.81 ± 3.0 vs $1.10 \pm 0.3 \mu g \text{ POC L}^{-1} \text{ d}^{-1}$ for on- and off-shelf stations, respectively).

30
31 Recent studies in the NESAP have estimated that photo-oxidation may account for 20–70 % of gross DMS removal in the
32 NESAP (Asher et al. 2017), and it is possible that this process is particularly important in offshore waters. Bouillon and Miller
33 (2004) found that quantum yields of DMS photo-oxidation in the NESAP correlated well to nitrate concentrations, suggesting
34 that this pathway is particularly relevant in the HNLC region where excess macronutrients persist throughout the summer.

1 Thus, the role of biological DMS consumption on influencing total DMS concentrations may be more important in the
2 generally low nitrate coastal waters.

3

4 [Rates of DMSPd turnover were among the highest measured anywhere, likely due, in part, to the very high productivity of the](#)
5 [waters we sampled.](#) However, no correlation was found between DMSPd loss rates or loss rate constants and DMS
6 concentrations in our study. This lack of correlation may be due, in part, to variation in DMSPd loss pathways. The DMS
7 yield of DMSP metabolism can vary significantly depending on metabolic needs of bacteria present, and relative abundance
8 of phytoplankton with DMSP lyase activity (Yoch 2002). [Although DMS yield was not measured in this study, previous](#)
9 [reports have shown that](#) in the NESAP, a low carbon to organic sulfur ratio in the HNLC regime results in increased DMS-
10 yield from DMSP metabolism, whereas onshore DMS-yield is relatively lower (Merzouk et al. 2006; Royer et al. 2010).
11 Further, variation in DMS loss processes may obscure a relationship between DMSPd cleavage and DMS concentrations, as
12 high loss terms may disproportionately impact net DMS production. We are currently investigating, in greater detail, the
13 patterns of DMS and DMSPd consumption from our O16 and O17 cruises (Kiene et al., in prep).

14 **4.4 Insights from merged data set**

15 Our merged data set, binned to 1° x 1° spatial resolution, builds on the L11 climatology to further constrain summertime DMS
16 distributions across the NESAP region. Despite an overall ~20 % increase in data-containing bins, and the inclusion of data
17 from seven additional years, we see only small changes in the derived climatological DMS concentrations and sea-air fluxes
18 when compared to the PMEL data set used by L11 (Table 3). Our new observations thus support the validity of the L11
19 climatology in the NESAP region, providing further confidence in the apparent distribution patterns, and a greater spatial
20 footprint for the climatological field. A significant result of our analysis is the presence of high DMS:chl-*a* in offshore waters
21 (Fig. 10c). [This result](#) builds on previous reports of higher DMSP:chl-*a* concentrations in offshore NESAP waters, and
22 [highlights](#) the importance of prymnesiophytes, [dinoflagellates](#), and other DMSP-rich phytoplankton taxa in driving DMS
23 accumulation in [this region](#).

24 **4.5 Biogeochemical provinces**

25 When examining results from our 1° binned data set, a separation of the NESAP into on- and off-shelf regimes does not capture
26 the biogeochemical complexities of the region. Ecological provinces, as defined by Longhurst (2007), define regions with
27 coherent seasonal trends in physical processes, which give rise to similar biological and chemical characteristics. The use of
28 Longhurst's biogeochemical provinces may thus be a more suitable (though still imperfect) approach to examine large-scale
29 and long-term differences in DMS cycling across the region. Work by Reygondeau et al. (2013) has demonstrated the potential
30 for shifts in province boundaries over time, including decrease of coastal province size during El Nino periods, and a general
31 shore-ward shift of ALSK boundaries during summer months. A model-based classification of marine ecosystems in the North
32 Pacific by Gregr and Bodtker (2007) divides our study region into six domains that show little similarity to Longhurst
33 provinces. It is difficult to say which of these classification schemes is most appropriate for examination of DMS dynamics.

1 However, [for the sake of direct comparison with L11](#), we [chose to use](#) Longhurst's provinces to examine regional cycling
2 differences (Hind et al. 2011; Belviso et al. 2011; Royer et al. 2015). While we acknowledge these provinces provide only a
3 crude [distinction](#) of biogeochemical regimes, they remain a best-approximation without delving into more complicated time-
4 resolved ecological province models (Reygondeau et al. 2013). Going forward, it may be useful to examine DMS dynamics
5 in sub-regions defined with a number of different metrics.

6 **4.6 Correlation with environmental variables**

7 Our analysis shows that no single variable can explain an appreciable amount of variability in DMS concentrations across the
8 NESAP. This result is consistent with previous global and regional studies (Kettle et al. 1999; Vézina 2004; Lana et al. 2011).
9 Nonetheless, an examination of the differing relationships between DMS concentrations and other environmental variables
10 provides insight into potential underlying factors driving DMS distribution (Table 4). For example, although we found a
11 moderately strong significant positive correlation between DMS and chl-*a* in the largely HNLC PSAE province, no relationship
12 [was](#) observed between these variables in the CCAL province. As noted above and confirmed in several previous studies, the
13 phytoplankton community structure in the offshore PSAE region consists largely of small, DMSP-rich species (Booth et al.
14 1993; Suzuki et al. 2002; Royer et al. 2010; Steiner et al. 2012), and large blooms are infrequent. Indeed, the average binned
15 chl-*a* concentration in this province is $< 1 \mu\text{g L}^{-1}$. As such, modest increases chl-*a* likely reflects a stimulation of this high
16 DMSP-producing community. The positive correlation with calcite (an indicator of high-DMSP producing coccolithophores)
17 supports this idea.

18
19 The relationship between chl-*a* and DMS is more complicated in the CCAL. High productivity in coastal upwelling zones
20 results in a strong onshore/offshore trend in average chl-*a* concentrations. Yet, no such trend is observed in DMS
21 concentrations. This may be due, in part, to the sensitivity of DMS concentrations to phytoplankton assemblage composition
22 and bloom dynamics. High phytoplankton biomass alone will not result in elevated DMS in this region. Rather, elevated
23 DMS concentrations may occur as a response to conditions of late-bloom nutrient stress, as discussed above [and in section 4.7](#).

24
25 Factors driving observed DMS distribution patterns in the ALSK province are more difficult to surmise. DMS is notably high
26 in the cold, productive waters adjacent to the Alaskan Peninsula. This is affirmed by a weak negative correlation between
27 DMS and SST, and the positive correlation between DMS and chl-*a*. Given that this portion of the province is known to
28 experience localized summer upwelling, it is possible that high DMS in the regions simply reflects elevated productivity [and](#)
29 [related upwelling-induced stressors](#).

30 **4.7 Algorithm performance**

31 Our results suggest that no single empirical algorithm is likely to perform well in predicting DMS distributions across the
32 subarctic Pacific, [although some predictive success was observed in the offshore waters of the CCAL province](#). Perhaps the
33 most informative result was the negative correlation between measured and modelled results using the VS07 algorithm. This

1 algorithm predicts DMS concentrations from solar radiative dose, a term that measures depth-integrated exposure to sunlight.
2 The underlying assumption in this algorithm is that increases in SRD are accompanied by increases in DMS due to UV-induced
3 oxidative stress (Vallina and Simó 2007). However, it is also possible that elevated SRD can also lead to a decrease in surface
4 water DMS concentrations through DMS photo-oxidation. As observed in previous studies, photo-oxidation in the NESAP
5 may account for up to 70 % of gross DMS removal, and rates are positively correlated with nitrate concentrations (Bouillon
6 and Miller 2004; Asher et al. 2017). Thus, in the high-nitrate NESAP, SRD may serve primarily to remove DMS from surface
7 waters, rather than stimulate DMS production, as suggested by the negative correlation between DMS and SRD across the
8 NESAP and within the PSAE province (Table 5). In areas with low surface water nitrate concentrations, such as the CCAL
9 province (Boyd and Harrison 1999), SRD could act to promote DMS accumulation. The good performance of the G18
10 algorithm in the CCAL province supports this idea. In contrast to the VS07 algorithm, G18 includes terms representing both
11 irradiance (PAR) and biology (DMSPt estimate), thus including the influence the combined effect of biomass and
12 phytoplankton physiological state. The poor performance of the G18 algorithm across other NESAP regions may be due to
13 the nitrate–photolysis relationship described above, or to the limited environmental-dependence of DMSP production in
14 prymnesiophyte / dinoflagellate-dominated HNLC phytoplankton (McParland and Levine 2018).

15
16 The results discussed above underline the need for regional algorithm tuning, and the selection of models best suited for a
17 given area and season. There is a particular need to develop approaches representing DMS distributions in HNLC regions. In
18 order to accomplish this goal, it will be important to improve mechanistic understanding of DMS/P dynamics, merging field-
19 based process studies with prognostic numerical models (e.g. Aumont et al. 2002, Clainche et al. 2004, Steiner et al. 2012,
20 Wang et al. 2015, Hayashida et al. 2016).

21 **5 Conclusion**

22 This study examines the distribution and cycling of DMS across the NESAP at various spatial scales. Our results confirm the
23 importance of high-DMSP producers (i.e. prymnesiophytes and dinoflagellates) to DMS accumulation in offshore waters,
24 while also demonstrating the importance of diatom-dominated assemblages in driving DMS distribution in coastal upwelling
25 regions. We further highlight the importance of metabolic rate processes in DMS distributions, providing evidence for the
26 importance of DMS consumption on concentration gradients at a fine-scale. On the short spatial scales covered by our transect
27 surveys, we observed strong correlations between DMS concentrations and other variables (i.e. SSHA, salinity). Over regional
28 scales, however, we only observed weak statistical relationships. All predictive algorithms we tested showed poor performance
29 in predicting DMS concentrations across the NESAP region, although performance was improved through the use of
30 regionally-tuned coefficients. Our compiled data set further support the importance of the NESAP as a global DMS ‘hot spot’
31 in summer, with patterns of DMS concentrations and sea–air fluxes similar to those observed in Lana et al.’s 2011 climatology.
32 Given the significance of the NESAP in global oceanic DMS emissions, future studies should seek to improve mechanistic

1 understanding of the factors driving DMS accumulation in this region, with the aim of predicting climate-dependent changes
2 over the coming decades.

3 **Code availability**

4 The codes used for spatial binning and data analysis can be provided by the authors upon request.

5 **Data availability**

6 All previously publicly unavailable DMS concentration data presented here have been submitted to the NOAA PMEL database
7 (<http://saga.pmel.noaa.gov/dms/>). Ancillary shipboard and satellite data can be provided by the authors upon request.

8 **Author contributions**

9 A. Herr compiled and analysed all data presented here, wrote all MATLAB codes, and wrote the manuscript, with editing and
10 intellectual input provided by P. Tortell R. Kiene and J. Dacey. R. Kiene further provided all biological rate measurement
11 data presented here, and J. Dacey assisted in collection of other field measurements.

12 **Competing interests**

13 The authors declare that they have no conflict of interest.

14 **Acknowledgements**

15 We dedicate this article to the memory of Dr. Ron Kiene, a wonderful scientist, mentor and friend. His contributions to DMS/P
16 research have shaped our field over the past three decades, and he will be missed by many around the world. We also wish to
17 thank many individuals involved in data collection and logistical aspects of the cruises presented here, including scientists
18 from the Institute of Ocean Sciences, the captain and crew of the R/V *Oceanus* and the CCGS *John P. Tully*, and members
19 Tortell, Kiene, Levine and Hatton laboratory groups. We also thank T. Ahlvin for GIS support, and both reviewers for their
20 insightful comments. Support for this work was provided from the US National Science Foundation (Grant #1436344), and
21 from the Natural Sciences and Engineering Research Council of Canada.

1 **References**

- 2 Asher, E. C., Merzouk, A., and Tortell, P. D.: Fine-scale spatial and temporal variability of surface water dimethylsulfide
3 (DMS) concentrations and sea-air fluxes in the NE Subarctic Pacific, *Mar. Chem.*, 126, 63–75,
4 doi:10.1016/j.marchem.2011.03.009, 2011.
- 5
- 6 [Asher, E. C., Dacey, J. W. H., Jarníková, T., Tortell, P. D.: Measurement of DMS, DMSO, and DMSP in natural waters by
7 automated sequential chemical analysis, *Limnol. Oceanogr.-Methods*, 13, 451–462, doi: 10.1002/lom3.10039, 2015.](#)
- 8
- 9 Asher, E., Dacey, J. W., Ianson, D., Peña, A., and Tortell, P.D.: Concentrations and cycling of DMS, DMSP, and DMSO in
10 coastal and offshore waters of the Subarctic Pacific during summer, 2010–2011, *J. Geophys. Res.-Oceans*, 122(4), 3269–3286,
11 doi:10.1002/2016JC012465, 2017.
- 12
- 13 Aumont, O., Belviso, S., and Monfray, P.: Dimethylsulfoniopropionate (DMSP) and dimethylsulfide (DMS) sea surface
14 distributions simulated from a global three-dimensional ocean carbon cycle model, *J. Geophys. Res.-Oceans*, 107, 3029,
15 doi:10.1029/1999JC000111, 2002.
- 16
- 17 Balch, W. M., Gordon, H. R., Bowler, B. C., Drapeau, D. T., and Booth, E. S.: Calcium carbonate measurements in the surface
18 global ocean based on Moderate-Resolution Imaging Spectroradiometer data, *J. Geophys. Res.-Oceans*, 110, C07001,
19 doi:10.1029/2004JC002560, 2005.
- 20 Barber, R. T. and Hiscock, M. R.: A rising tide lifts all phytoplankton: Growth response of other phytoplankton taxa in diatom-
21 dominated blooms, *Global Biogeochem. Cycles*, 20, 1–12, doi:10.1029/2006GB002726, 2006.
- 22 Barnard, W. R., Andreae, M. O., and Iverson, R. L.: Dimethylsulfide and *Phaeocystis poucheti* in the southeastern Bering Sea,
23 *Cont. Shelf Res.*, 3, 103–113, doi: 10.1016/0278-4343(84)90001-3, 1984.
- 24
- 25 Belviso, S., Kim, S.-K., Rassoulzadegan, B., Krajka, B., Nguyen, B. C., Mihalopoulos, N., and Buat-Menard, P.: Production
26 of dimethylsulfonium propionate (DMSP) and dimethylsulfide (DMS) by a microbial food web, *Limnol. Oceanogr.* 35, 1810–
27 1821, doi: 10.4319/lo.1990.35.8.1810, 1990.
- 28 Belviso, S., Sciandra, A. and Copin-Montégut, C.: Mesoscale features of surface water DMSP and DMS concentrations in the
29 Atlantic Ocean off Morocco and in the Mediterranean Sea, *Deep. Res. Part I Oceanogr. Res. Pap.*, 50, 543–555,
30 doi:10.1016/S0967-0637(03)00032-3, 2003.

- 1 Belviso, S., Masotti, I., Tagliabue, A., Bopp, L., Brockmann, P., Fichot, C., Caniaux, G., Prieur, L., Ras, J., Uitz, J., Loisel,
2 H., Dessailly, D., Alvain, S., Kasamatsu, N., and Fukuchi, M.: DMS dynamics in the most oligotrophic subtropical zones of
3 the global ocean, *Biogeochemistry*, 110, 215–241, doi:10.1007/s10533-011-9648-1, 2012.
- 4
- 5 Booth, B., Lewin, J., and Postel, J.: Temporal variation in the structure of autotrophic and heterotrophic communities in the
6 subarctic Pacific, *Prog. Oceanogr.*, 32, 57–99, doi:10.1016/0079-6611(93)90009-3, 1993.
- 7
- 8 Bouillon, R.-C., and Miller, W. L.: Determination of apparent quantum yield spectra of DMS photo-degradation in an in situ
9 iron-induced Northeast Pacific Ocean bloom, *Geophys. Res. Lett.*, 31, L06310, doi:10.1029/2004GL019536, 2004.
- 10
- 11 Boyd, P. J. and Harrison, P. J.: Phytoplankton dynamics in the NE subarctic Pacific, *Deep-sea Res. Pt. I.*, 46, 2405–2432,
12 doi:10.1016/S0967-0645(99)00069-7, 1999.
- 13
- 14 Boyd, P. W., Law, C. S., Wong, C. S., Nojiri, Y., Tsuda, A., Levasseur, M., Takeda, S., Rivkin, R., Harrison, P. J., Strzepek,
15 R., Gower, J., McKay, M., Abraham, E., Arychuk, M., Barwell-Clarke, J., Crawford, W., Crawford, D., Hale, M., Harada, K.,
16 Johnson, K., Kiyosawa, H., Kudo, I., Marchetti, A., Miller, W., Needoba, J., Nishioka, J., Ogawa, H., Page, J., Robert, M.,
17 Saito, H., Sastri, A., Sherry, N., Soutar, T., Sutherland, N., Taira, Y., Whitney, F., Wong, S.-K. E., and Yoshimura, T.: The
18 decline and fate of an iron-induced subarctic phytoplankton bloom, *Nature* 428, 549–553, doi:10.1038/nature02412, 2004.
- 19
- 20 Brewin, R., Sathyendranath, S., Hirata, T., Lavender, S., Barciela, R., and Hardman-Mountford, N.: A three-component model
21 of phytoplankton size class for the Atlantic Ocean, *Ecol. Model.*, 221, 1472–1483, doi:10.1016/j.ecolmodel.2010.02.014,
22 2010.
- 23
- 24 Bricaud, A., Babin, M., Morel, A. and Claustre, H.: Variability in the chlorophyll-specific absorption coefficients of natural
25 phytoplankton: Analysis and parameterization, *J. Geophys. Res.-Oceans*, 100, 13321–13332, doi:10.1029/95JC00463, 1995.
- 26
- 27 Bucciarelli, E., and Sunda, W.: Influence of CO₂, nitrate, phosphate, and silicate limitation on intracellular
28 dimethylsulfoniopropionate in batch cultures of the coastal diatom *Thalassiosira pseudonana*, *Limnol. Oceanogr.*, 48, 2256–
29 2265, doi:10.4319/lo.2003.48.6.2256, 2003.
- 30
- 31 Bucciarelli, E., Ridame, C., Sunda, W., Dimier-Hugueney, C., Cheize, M., and Belviso, S.: Increased intracellular
32 concentrations of DMSP and DMSO in iron-limited oceanic phytoplankton *Thalassiosira oceanica* and *Trichodesmium*
33 *erythraeum*, *Limnol. Oceanogr.*, 58, 1667–1679, doi:10.4319/lo.2013.58.5.1667, 2013.
- 34

- 1 Burt, W., Westberry, T., Behrenfeld, M., Zeng, C., Izett, R., Tortell, P.: Carbon: Chlorophyll Ratios and Net Primary
2 Productivity of Subarctic Pacific Surface Waters Derived From Autonomous Shipboard Sensors, *Global Biogeochem. Cy.*, 32,
3 267–288, doi:10.1002/2017GB005783, 2018.
- 4
- 5 Charlson, R. J., Lovelock, J. E., Andreae, M. O. and Warren, S. G.: Oceanic phytoplankton, atmospheric sulphur, cloud albedo
6 and climate, *Nature*, 326, 655–661, doi:10.1038/326655a0, 1987.
- 7
- 8 Clainche, Y. L., Levasseur, M., Vézina, A., Dacey, J. W. H., and Saucier, F. J.: Behaviour of the ocean DMS (P) pools in the
9 Sargasso Sea viewed in a coupled physical-biogeochemical ocean model, *Can. J. Fish. Aquat. Sci.*, 61, 788–803,
10 doi:10.1139/F04-027, 2004.
- 11
- 12 Crawford, W., Brickley, P., Peterson, T., and Thomas, A.: Impact of Haida Eddies on chlorophyll distribution in the Eastern
13 Gulf of Alaska, *Deep-Sea Res. Pt. II*, 52, 975–989, doi:10.1016/j.dsr2.2005.02.011, 2005.
- 14
- 15 Curson, A., Williams, B., Pinchbeck, B., Sims, L., Martínez, A., Rivera, P., Kumaresan, D., Mercadé E., Spurgin, L., Carrión
16 O., Moxon S., Cattolico, R., Kuzhiumparambil, U., Guagliardo, P., Clode, P., Raina, J.-B., and Todd, J.: DSYB catalyses the
17 key step of dimethylsulfoniopropionate biosynthesis in many phytoplankton, *Nat. Microbiol.*, 3, 430–439,
18 doi:10.1038/s41564-018-0119-5, 2018.
- 19
- 20 Dacey, J. W., and Blough, N. V.: Hydroxide decomposition of dimethylsulfoniopropionate to form dimethylsulfide, *Geophys.*
21 *Res. Lett.*, 14, 1246–1249, doi:10.1029/GL014i012p01246, 1987.
- 22
- 23 Dacey, J. W. H, and Wakeham, S. G.: Oceanic dimethylsulfide: production during zooplankton grazing on phytoplankton,
24 *Science*, 233, 1314–1316, doi: 10.1126/science.233.4770.1314, 1986.
- 25
- 26 Ducklow, H., Dickson, M.-L., Kirchman, D., Steward, G., Orchardo, J., Marra, J., and Azam, F.: Constraining bacterial
27 production, conversion efficiency and respiration in the Ross Sea, Antarctica, January-February 1997. *Deep-Sea Res. II*, 47,
28 3227-3247, doi: 10.1016/S0967-0645(00)00066-7, 2000.
- 29
- 30 Franklin, D. J., Poulton, A. J., Steinke, M., Young, J., Peeken, I., and Malin, G.: Dimethylsulphide, DMSP-lyase activity and
31 microplankton community structure inside and outside of the Mauritanian upwelling, *Prog. Oceanogr.*, 83, 134–142,
32 doi:10.1016/j.pocean.2009.07.011, 2009.
- 33 Frouin, R., Franz, B. and Wang, M.: Algorithm to estimate PAR from SeaWiFS data Version 1.2-Documentation., 2003.

- 1 Gabric, A. J., Matrai, P. A., and Vernet, M.: Modelling the production and cycling of dimethylsulphide during the vernal bloom
2 in the Barents Sea, *Tellus*, 51B, 919-937, doi: /10.3402/tellusb.v51i5.16505, 1999.
- 3 Galí, M. and Simó, R.: A meta-analysis of oceanic DMS and DMSP cycling processes: Disentangling the summer paradox,
4 *Global Biogeochem. Cycles*, 29, 496–515, doi:10.1002/2014GB004940, 2015.
- 5 Galí, M., Devred, E., Levasseur, M., Royer, S.-J., and Babin, M.: A remote sensing algorithm for planktonic
6 dimethylsulfoniopropionate (DMSP) and an analysis of global patterns, *Remote Sens. Environ.*, 171, 171–184,
7 doi:10.1016/j.rse.2015.10.012, 2015.
- 8 Galí, M., Levasseur, M., Devred, E., Simó, R., and Babin, M.: Sea-surface dimethylsulfide (DMS) concentration from satellite
9 data at global and regional scales, *Biogeosciences*, 15, 3497–3519, doi:10.5194/bg-2018-18, 2018.
- 10
- 11 Goes, J., Saino, T., Oaku, H., Ishizaka, J., Wong, C., and Nojiri, Y: Basin scale estimates of sea surface nitrate and new
12 production from remotely sensed sea surface temperature and chlorophyll, *Geophys. Res. Lett.*, 27, 1263–1266,
13 doi:10.1029/1999GL002353, 2000.
- 14
- 15 Gordon, H. R., Boynton, G. C., Balch, W. M., Groom, S. B., Harbour, D. S., and Smyth, T. J.: Retrieval of coccolithophore
16 calcite concentration from SeaWiFS imagery, *Geophys. Res. Lett.*, 28, 1587–1590, doi:10.1029/2000GL012025, 2001.
- 17
- 18 Gregr, E., and Bodtke, K.: Adaptive classification of marine ecosystems: Identifying biologically meaningful regions in the
19 marine environment, *Deep-Sea Res. Pt. I*, 54, 385–402, doi:10.1016/j.dsr.2006.11.004, 2007.
- 20
- 21 Harada, H., Vila-Costa, M., Cebrian, J., and Kiene, R.: Effects of UV radiation and nitrate limitation on the production of
22 biogenic sulfur compounds by marine phytoplankton, *Aquat. Bot.*, 90, 37–42, doi:10.1016/j.aquabot.2008.05.004, 2009.
- 23
- 24 Hatton, A. D., Turner, S. M., Malin, G., and Liss, P. S.: Dimethylsulphoxide and other biogenic sulphur compounds in the
25 Galapagos Plume, *Deep-Sea Res. Pt. II*, 45, 1043–1053, doi:10.1016/S0967-0645(98)00017-4, 1998.
- 26
- 27 Hatton, A. D. Malin G., and Liss, P.S., Distribution of biogenic sulphur compounds during and just after the southwest
28 monsoon in the Arabian Sea, *Deep-Sea Res. Pt. II*, 46, 617–632, doi:10.1016/S0967-0645(98)00120-9, 1999.
- 29
- 30 Hayashida, H., Steiner, N., Monohan, A., Galindo, V., Lizotte, M., and Levasseur, M.: Implications of sea-ice biogeochemistry
31 for oceanic production and emissions of dimethyl sulfide in the Arctic, *Biogeosciences*, 14, 3129–3155, 2017.
- 32

- 1 Hill, R. W., White, B. A., Cottrell, M. T., and Dacey, J. W. H.: Virus-mediated total release of dimethylsulfoniopropionate
2 from marine phytoplankton: a potential climate process, *Aquat. Microb. Ecol.*, 14: 1–6, doi: 10.3354/ame014001, 1998.
3
- 4 Hind, A. J., Rauschenberg, C. D., Johnson, J. E., Yang, M., Matrai, P. A.: The use of algorithms to predict surface seawater
5 dimethyl sulphide concentrations in the SE Pacific, a region of steep gradients in primary productivity, biomass and mixed
6 layer depth, *Biogeosciences*, 8, 1–16, doi:10.5194/bg-8-1-2011, 2011.
7
- 8 Hirata, T., Aiken, J., Hardman-Mountford, N., Smyth, T. J., and Barlow, R. G.: An absorption model to determine
9 phytoplankton size classes from satellite ocean colour, *Remote Sens. Environ.*, 112, 3153–3159,
10 doi:10.1016/j.rse.2008.03.011, 2008.
11
- 12 Hirata, T., Hardman-Mountford, N. J., Brewin, R. J., Aiken, J., Barlow, R., Suzuki, K., Isada, T., Howell, E., Hashioka, T.,
13 Noguchi-Aita, M., and Yamanaka, Y.: Synoptic relationships between surface Chlorophyll-a and diagnostic pigments specific
14 to phytoplankton functional types, *Biogeosciences*, 8, 311–327, doi:10.5194/bg-8-311-2011, 2011.
15
- 16 Hockin, N. L., Mock, T., Mulholland, F., Kopriva, S., and Malin, G.: The response of diatom central carbon metabolism to
17 nitrogen starvation is different from that of green algae and higher plants, *Plant Physiol.*, 158, 299–312,
18 doi:10.1104/pp.111.184333, 2012.
19
- 20 Holligan, P. M., Turner, S. M., and Liss, P. S.: Measurements of dimethyl sulphide in frontal regions, *Cont. Shelf Res.*, 7, 213-
21 224, doi: 10.1016/0278-4343(87)90080-X, 1987.
- 22 Hu, C., Lee, Z. and Franz, B.: Chlorophyll *a* algorithms for oligotrophic oceans: A novel approach based on three-band
23 reflectance difference, *J. Geophys. Res.*, 117(C1), C01011, doi:10.1029/2011JC007395, 2012.
- 24 Izett, R. W., Manning, C. C., Hamme, R. C., and Tortell, P. D.: Refined Estimates of Net Community Production in the
25 Subarctic Northeast Pacific Derived From $\Delta O_2/Ar$ Measurements With N_2O -Based Corrections for Vertical Mixing, *Global*
26 *Biogeochem. Cy.*, 32, 326–350, doi:10.1002/2017GB005792, 2018.
27
- 28 Jarníková, T., Dacey, J., Lizotte, M., Levasseur, M., and Tortell, P.: The distribution of methylated sulfur compounds, DMS
29 and DMSP, in Canadian subarctic and Arctic marine waters during summer 2015, *Biogeosciences*, 15, 2449–2465,
30 doi:10.5194/bg-15-2449-2018, 2018.
31
- 32 Jarníková, T., and Tortell, P. D.: Towards a revised climatology of summertime dimethylsulfide concentrations and sea–air
33 fluxes in the Southern Ocean, *Environ. Chem.*, 13, 364–378, doi:10.1071/EN14272, 2016.

1
2 Johnson, K., Miller, L., Sutherland, N., and Wong, C. S.: Iron transport by mesoscale Haida eddies in the Gulf of Alaska,
3 *Deep-Sea Res. Pt. II*, 52, 933–953, doi:10.1016/j.dsr2.2004.08.017, 2005.
4
5 Johnson, W., Soule, M., and Kujawinski, E.: Evidence for quorum sensing and differential metabolite production by a marine
6 bacterium in response to DMSP, *ISME J.*, 10, 2304–2316, doi:10.1038/ismej.2016.6, 2016.
7
8 Kaiser, J., Reuer, M. K., Barnett, B., and Bender, M. L.: Marine productivity estimates from continuous O₂/Ar ratio
9 measurements by membrane inlet mass spectrometry, *Geophys. Res. Lett.*, 32, L19605, doi:10.1029/2005GL023459, 2005.
10
11 Keller, M. D.: Dimethyl Sulfide Production and Marine Phytoplankton: The Importance of Species Composition and Cell Size,
12 *Biol. Oceanogr.*, 6, 375–382, doi:10.1080/01965581.1988.10749540, 1989.
13
14 Kettle, A. J., Andreae, M. O., Amouroux, D., Andreae, T. W., Bates, T. S., Berresheim, H., Bingemer, H., Boniforti, R., Curran,
15 M. A., DiTullio, G. R., Helas, G., Jones, G. B., Keller, M. D., Kiene, R. P., Leck, C., Levasseur, M., Malin, G., Maspero, M.,
16 Matrai, P., McTaggart, A. R., Mihalopoulos, N., Nguyen, B. C., Novo, A., Putaud, J. P., Rapsomanikis, S., Roberts, G.,
17 Schebeske, G., Sharma S., Simó, R., Staubes, R., Turner, S., and Uher, G.: A global database of sea surface dimethylsulfide
18 (DMS) measurements and a procedure to predict sea surface DMS as a function of latitude, longitude, and month, *Global*
19 *Biogeochem. Cy.*, 13, 399–444, doi:10.1029/1999GB900004, 1999.
20
21 Kiene, R. P., and Linn, L. J.: Distribution and turnover of dissolved DMSP and its relationship with bacterial production and
22 dimethylsulfide in the Gulf of Mexico, *Limnol. Oceanogr.*, 45, 849–861, doi:10.4319/lo.2000.45.4.0849, 2000.
23
24 Kiene, R.P., and Service, S.: Decomposition of dissolved DMSP and DMS in estuarine waters: dependence on temperature
25 and substrate concentration., *Mar. Ecol. Prog. Ser.*, 76, 1–11, doi:10.3354/meps076001, 1991.
26
27 Kiene, R. P., and Slezak, D.: Low dissolved DMSP concentrations in seawater revealed by small-volume gravity filtration and
28 dialysis sampling, *Limnol. Oceanogr.-Meth.*, 4, 80–95, doi:10.4319/lom.2006.4.80, 2006.
29
30 Kiene, R. P., Linn, L. J., and Bruton, J. A.: New and important roles for DMSP in marine microbial communities, *J. Sea. Res.*,
31 43, 209–224, doi:10.1016/S1385-1101(00)00023-X, 2000.

32 Kiene, R. P., Kieber, D. J., Slezak, D., Toole, D. A., Valle, D. del, Bisgrove, J., Brinkley, J. and Rellinger, A.: Distribution
33 and cycling of dimethylsulfide, dimethylsulfoniopropionate, and dimethylsulfoxide during spring and early summer in the
34 Southern Ocean south of New Zealand, *Aquat. Sci.*, 69, 305–319, doi:10.1007/s00027-007-0892-3, 2007.

- 1 Kinsey, J. D., Kieber, D. J., Neale, P. J.: Effects of iron limitation and UV radiation on *Phaeocystis antarctic* growth and
2 dimethylsulfoniopropionate, dimethylsulfoxide and acrylate concentrations, *Environ. Chem.*, 13, 195–211,
3 doi:10.1071/EN14275, 2016.
- 4 Lam, P. J., and Letters, J.K.: The continental margin is a key source of iron to the HNLC North Pacific Ocean, *Geophys. Res.*
5 *Let.*, 35, L07608, doi:10.1029/2008GL033294, 2008.
- 6
- 7 Lana, A., Bell, T. G., Simó, R., Vallina, S. M., Ballabrera-Poy, J., Kettle, A. J., Dachs, J., Bopp, L., Saltzman, E. S., Stefels,
8 J., Johnson, J. E., and Liss, P. S.: An updated climatology of surface dimethylsulfide concentrations and emission fluxes in
9 the global ocean, *Global Biogeochem. Cy.*, 25, GB1004, doi:10.1029/2010GB003850, 2011.
- 10
- 11 Levasseur, M., Gosselin, M., Michaud, S.: A new source of dimethylsulfide (DMS) for the arctic atmosphere: ice diatoms,
12 *Mar. Biol.*, 121, 381–387, doi:10.1007/BF00346748, 1994.
- 13
- 14 Levasseur, M., Michaud, S., Egge, J., Cantin, G., Nejstgaard, J. C., Sanders, R., Fernandez, E., Solberg, P. T., Heimdal, B.,
15 and Gosselin, M.: Production of DMSP and DMS during a mesocosm study of an *Emiliania huxleyi* bloom: influence of
16 bacteria and *Calanus finmarchicus* grazing, *Mar. Biol.*, 126, 609–618, doi:10.1007/BF00351328, 1996.
- 17
- 18 Levasseur, M., Scarratt, M. G., Michaud, S., Merzouk, A., Wong, C., Arychuk, M., Richardson, W., Rivkin, R. B., Hale, M.,
19 Wong, E., Marchetti, A., and Kiyosawa, H.: DMSP and DMS dynamics during a mesoscale iron fertilization experiment in
20 the Northeast Pacific—Part I: Temporal and vertical distributions, *Deep-Sea Res.*, Pt. II 53, 2353–2369,
21 doi:10.1016/j.dsr2.2006.05.023, 2006.
- 22
- 23 Levine, N. M., Toole, D. A., Neeley, A., Bates, N. R., Doney, S. C., Dacey, J. W. H.: Revising upper-ocean sulfur dynamics
24 near Bermuda: new lessons from 3 years of concentration and rate measurements, *Environ. Chem.*, 13, 302–313,
25 doi:10.1071/EN15045, 2016.
- 26
- 27 Li, H., Liu, Z., Xu, J., Wu, X., Chaohui, S., Lu, S., and Minjie, C.: Manual of Global Ocean Argo gridded data set (BOA-
28 Argo) (Version 2017), 2017.
- 29
- 30 Locarnini, S., Turner, S. and Liss, P.: The distribution of dimethylsulfide, DMS, and dimethylsulfoniopropionate, DMSP, in
31 waters off the Western Coast of Ireland, *Cont. Shelf Res.*, 18, 1455–1473, doi:10.1016/S0278-4343(98)00035-1, 1998.
- 32
- 33 Longhurst, A. R.: *Ecological Geography of the Sea*, 2nd ed. Elsevier, doi:10.1016/B978-0-12-455521-1.X5000-1, 2007.
- 34

- 1 Lovelock, J., Maggs, R., and Rasmussen, R.: Atmospheric dimethyl sulphide and the natural sulphur cycle, *Nature*, 237, 452–
2 453, doi:10.1038/237452a0. 1972.
- 3
- 4 Malin, G., Turner, S., Liss, P., Holligan, P., and Harbour, D.: Dimethylsulphide and dimethylsulphonioacetate in the
5 Northeast Atlantic during the summer coccolithophore bloom, *Deep-Sea Res. Pt. I*, 40, 1487–1508, doi:10.1016/0967-
6 0637(93)90125-M, 1993.
- 7
- 8 Matrai, P. A. and Keller, M. D.: Dimethylsulfide in a large-scale coccolithophore bloom in the Gulf of Maine, *Cont. Shelf*
9 *Res.*, 13, 831–843, doi:10.1016/0278-4343(93)90012-M, 1993.
- 10
- 11 Matrai, P. A., and Vernet, M.: Dynamics of the vernal bloom in the marginal sea ice zone of the Barents Sea: Dimethyl sulphide
12 and dimethylsulphonioacetate budgets, *J. Geophys. Res.*, 102, 22965–22979, doi: 10.1029/96JC03870, 1997.
- 13
- 14 McParland, E. [L.](#) and Levine, N. [M.](#): The role of differential DMSP regulation and community composition in predicting
15 variability of global surface DMSP concentrations, *Limnol. Oceanogr.*, [doi:10.1002/lno.11076, 2018.](#)
- 16
- 17 Merzouk, A., Levasseur, M., Scarratt, M. G., Michaud, S., Rivkin, R. B., Hale, M. S., Kiene, R. P., Price, N. M., and Li, W.:
18 DMSP and DMS dynamics during a mesoscale iron fertilization experiment in the Northeast Pacific—Part II: Biological
19 cycling, *Deep-Sea Res. Pt. II*, 53, 2370–2383, doi:10.1016/j.dsr2.2006.05.022, 2006.
- 20
- 21 Nemcek, N., Ianson, D., and Tortell, P.: A high-resolution survey of DMS, CO₂, and O₂/Ar distributions in productive coastal
22 waters, *Global Biogeochem. Cy.*, 22, GB2009, doi:10.1029/2006GB002879, 2008.
- 23
- 24 O'Reilly, J. E., Maritorena, S., Mitchell, B. G., Siegel, D. A., Carder, K. L., Garver, S. A., Kahru, M. and McClain, C.: Ocean
25 color chlorophyll algorithms for SeaWiFS, *J. Geophys. Res.*, 103(C11), 24937–24953, doi:10.1029/98JC02160, 1998.
- 26
- 27 Reisch, C. R., Stoudemayer, M. J., Varaljay, V. A., Amster, I. J., Moran, M. A., and Whitman, W.: Novel pathway for
28 assimilation of dimethylsulphonioacetate widespread in marine bacteria, *Nature*, 473, 208–211, doi:10.1038/nature10078,
29 2011.
- 30
- 31 Reuer, M., Barnett, B., Bender, M., Falkowski, P., and Hendricks, M.: New estimates of Southern Ocean biological production
32 rates from O₂/Ar ratios and the triple isotope composition of O₂, *Deep-Sea Res. Pt. I*, 54, 951–974,
doi:10.1016/j.dsr.2007.02.007, 2007.

1 Reygondeau, G., Longhurst, A., Martinez, E., Beaugrand, G., Antoine, D., and Maury, O.: Dynamic biogeochemical provinces
2 in the global ocean, *Global Biogeochem. Cy.*, 27, 1046–1058, doi:10.1002/gbc.20089, 2013.

3

4 Ribalet, F., Marchetti, A., Hubbard, K., Brown, K., Durkin, C., Morales, R., Robert, M., Swalwell, J., Tortell, P., and Armbrust,
5 V.: Unveiling a phytoplankton hotspot at a narrow boundary between coastal and offshore waters, *P. Natl. A. Sci. USA*, 107,
6 16571–16576, doi:10.1073/pnas.1005638107, 2010.

7

8 Roesler, C., and Barnard, A.: Optical proxy for phytoplankton biomass in the absence of photophysiology: Rethinking the
9 absorption line height, *Methods in Oceanography*, 7, 79–94, doi:10.1016/j.mio.2013.12.003, 2013.

10

11 Royer, S.-J., Levasseur, M., Lizotte, M., Arychuk, M., Scarratt, M., Wong, C., Lovejoy, C., Robert, M., Johnson, K., Peña, A.,
12 Michaud, S., and Kiene, R.: Microbial dimethylsulfoniopropionate (DMSP) dynamics along a natural iron gradient in the
13 northeast subarctic Pacific, *Limnol. Oceanogr.*, 55, 1614–1626, doi:10.4319/lo.2010.55.4.1614, 2010.

14

15 [Royer, S. -J., Mahajan, A. S., Gali, M., Saltzman, E., and Simó, R: Small-scale variability patterns of DMS and phytoplankton
16 in surface waters of the tropical and subtropical Atlantic, Indian and Pacific Oceans, *Geophys. Res. Let.*, 42, 475–483,
17 doi:10.1002/2014GL062543, 2015.](#)

18

19 Saltzman, E. S., King, D. B., Holmen, K., and Leck, C.: Experimental determination of the diffusion coefficient of
20 dimethylsulfide in water, *J. Geophys. Res.*, 98, 16481–16468, doi:10.1029/93JC01858, 1993.

21

22 Saraceno, M., Strub, P. T., and Kosro, P. M.: Estimates of sea surface height and near-surface alongshore coastal currents from
23 combinations of altimeters and tide gauges, *J. Geophys. Res.-Oceans*, 113, C11013, doi:10.1029/2008JC004756, 2008.

24

25 Schuback, N., Schallenberg, C., Duckham, C., Maldonado, M. and Tortell, P.: Interacting Effects of Light and Iron Availability
26 on the Coupling of Photosynthetic Electron Transport and CO₂-Assimilation in Marine Phytoplankton, *Plos One*, 10:
27 e0133235, doi:10.1371/journal.pone.0133235, 2015.

28

29 Seymour, J. R., Simó, R., Ahmed, T., and Stocker, R.: Chemoattraction to Dimethylsulfoniopropionate Throughout the Marine
30 Microbial Food Web, *Science*, 329, 342–345, doi:10.1126/science.1188418, 2010.

31

32 Simó, R.: From cells to globe: approaching the dynamics of DMS (P) in the ocean at multiple scales, *Can. J. Fish. Aquat. Sci.*,
33 61, 673–684, doi:10.1139/f04-030, 2004.

34

- 1 Simó, R., and Dachs, J.: Global ocean emission of dimethylsulfide predicted from biogeophysical data, *Global Biogeochem.*
2 *Cy.*, 16, 1078, doi:10.1029/2001GB001829, 2002.
- 3 Simó, R., Saló, V., Almeda, R., Movilla, J., Trepát, I., Saiz, E. and Calbet, A.: The quantitative role of microzooplankton
4 grazing in dimethylsulfide (DMS) production in the NW Mediterranean, *Biogeochemistry*, 2, 1–18, doi:10.1007/s10533-018-
5 0506-2, 2018.
- 6 Simon, M., and Azam, F.: Protein content and protein synthesis rates of planktonic marine bacteria. *Mar. Ecol. Prog. Ser.*, 51,
7 201-213, doi: 10.3354/meps051201, 1989.
8
- 9 Smith, D., and Azam, F.: A simple, economical method for measuring bacterial protein synthesis rates in seawater using ³H-
10 leucine, *Marine Microbial Food Webs*, 6, 107–114, 1992.
11
- 12 Smith, R. L.: A description of current, wind, and sea level variations during coastal upwelling off the Oregon coast, July–
13 August 1972, *J. Geophys. Res.*, 79, doi:10.1029/JC079i003p00435, 1974.
14
- 15 [Stefels, J., van Boekel, W. H. M., Production of DMS from dissolved DMSP in axenic cultures of the marine phytoplankton](#)
16 [species *Phaeocystis* sp. *Mar. Ecol. Prog. Ser.*, 97, 11–18, doi:10.3354/meps097011, 1993.](#)
17
- 18 Stefels, J., Steinke, M., Turner, S., Malin, G., and Belviso, S.: Environmental constraints on the production and removal of the
19 climatically active gas dimethylsulphide (DMS) and implications for ecosystem modelling, *Biogeochemistry*, 83, 245–275,
20 doi:10.1007/s10533-007-9091-5, 2007.
21
- 22 Steiner, N., Robert, M., Arychuk, M., Levasseur, M., Merzouk, A., Peña, A., Richardson, W. and Tortell, P.: Evaluating DMS
23 measurements and model results in the Northeast subarctic Pacific from 1996–2010, *Biogeochemistry*, 110, 269–285,
24 doi:10.1007/s10533-011-9669-9, 2012.
25
- 26 Steinke, M., Malin, G., Archer, S. D., Burkill, P. H., and Liss, P. S.: DMS production in a coccolithophorid bloom: evidence
27 for the importance of dinoflagellate DMSP lyases, *Aquat. Microb. Ecol.*, 26, 259–270, doi:10.3354/ame026259, 2002.
28
- 29 Strub, T., and James, C.: The large-scale summer circulation of the California Current, *Geophys. Res. Lett.*, 22, 207–210,
30 doi:10.1029/94GL03011, 1995.
31
- 32 Sunda, W., Kieber, D. J., Kiene, R. P., and Huntsman, S.: An antioxidant function for DMSP and DMS in marine algae, *Nature*,
33 418, 317-320, doi:10.1038/nature00851, 2002.

1
2 Sunda, W., Hardison, R., Kiene, R., and Bucciarelli, E.: The effect of nitrogen limitation on cellular DMSP and DMS release
3 in marine phytoplankton: climate feedback implications, *Aquat. Sci.*, 69, 341–351, doi:10.1007/s00027-007-0887-0, 2007.
4
5 Suzuki, K., Minami, C., Liu, H., and Saino, T.: Temporal and spatial patterns of chemotaxonomic algal pigments in the
6 subarctic Pacific and the Bering Sea during the early summer of 1999, *Deep-Sea Res. Part II*, 49, 5685–5704,
7 doi:10.1016/s0967-0645(02)00218-7, 2002.
8
9 Sweeney, C., Gloor, E., Jacobson, A. R., Key, R. M., McKinley, G., Sarmiento, J. L., and Wanninkhof, R.: Constraining global
10 air-sea gas exchange for CO₂ with recent bomb ¹⁴C measurements, *Global Biogeochem. Cy.*, 21, GB2015,
11 doi:10.1029/2006gb002784, 2007.
12
13 Tabata, S., Thomas, B. and Ramsden, D.: Annual and interannual variability of steric sea level along line P in the northeast
14 Pacific Ocean, *J. Phys. Oceanogr*, 16, 1378–1398, doi:10.1175/1520-0485(1986)016<1378:AAIVOS>2.0.CO, 1986.
15
16 Tortell, P. D.: Dissolved gas measurements in oceanic waters made by membrane inlet mass spectrometry, *Limnol. Oceanogr.-*
17 *Meth.*, 3, 24–37, doi:10.4319/lom.2005.3.24, 2005a.
18
19 Tortell, P. D.: Small-scale heterogeneity of dissolved gas concentrations in marine continental shelf waters, *Geochem. Geophys.*
20 *Geosy.*, 6, Q11M04, doi:10.1029/2005GC000953, 2005b.
21
22 Turner, S. M., Nightingale, P. D., Broadgate, W., and Liss, P. S.: The distribution of dimethyl sulphide and
23 dimethylsulphoniopropionate in Antarctic waters and sea ice, *Deep-Sea Res. Pt. II*, 42, 1059–1080, doi:10.1016/0967-
24 0645(95)00066-Y, 1995.
25
26 Uitz, J., Claustre, H., Morel, A., and Hooker, S. B.: Vertical distribution of phytoplankton communities in open ocean: An
27 assessment based on surface chlorophyll, *J. Geophys. Res.-Oceans*, 111, C08005, doi:10.1029/2005JC003207, 2006.
28
29 Del Valle, D. A., Kieber, D. J., Toole, D. A., Brinkley, J., and Kiene, R. P.: Biological consumption of dimethylsulfide (DMS)
30 and its importance in DMS dynamics in the Ross Sea, Antarctica, *Limnol. Oceanogr.*, 54, 785–798,
31 doi:10.4319/lo.2009.54.3.0785, 2009.
32
33 Vallina, S., and Simó, R.: Strong relationship between DMS and the solar radiation dose over the global surface ocean, *Science*
34 315, 506–508, doi:10.1126/science.1133680, 2007.

- 1 Van Heukelem, L., Thomas, C. S.: Computer-assisted high-performance liquid chromatography method development with
2 applications to the isolation and analysis of phytoplankton pigments, *J. Chromatogr. A* 910, 31–49, doi:10.1016/S0378-
3 4347(00)00603-4, 2001.
- 4 Venegas, R. M., Strub, P. T., Beier, E., Letelier, R., Thomas, A. C., Cowles, T., James, C., Soto-Mardones, L., and Cabrera,
5 C.: Satellite-derived variability in chlorophyll, wind stress, sea surface height, and temperature in the northern California
6 Current System, *J. Geophys. Res.-Oceans* 113, C03015, doi:10.1029/2007JC004481, 2008.
7
- 8 Vézina, A.: Ecosystem modelling of the cycling of marine dimethylsulfide: a review of current approaches and of the potential
9 for extrapolation to global scales, *Can. J. Fish. Aquat. Sci.*, 61, 845–856, doi:10.1139/f04-025, 2004.
10
- 11 Vidussi, F., Claustre, H., Manca, B. B., Luchetta, A., and Marty, J.-C.: Phytoplankton pigment distribution in relation to upper
12 thermocline circulation in the eastern Mediterranean Sea during winter, *J. Geophys. Res.-Oceans*, 106,
13 doi:10.1029/1999JC000308, 19939–19956, 2001.
14
- 15 Vila-Costa, M., Kiene, R., and Simó, R.: Seasonal variability of the dynamics of dimethylated sulfur compounds in a coastal
16 northwest Mediterranean site, *Limnol. Oceanogr.*, 53, doi:10.4319/lo.2008.53.1.0198, 198–211, 2008.
17
- 18 Wang, S., Elliott, S., Maltrud, M., and Cameron-Smith, P.: Influence of explicit *Phaeocystis* parameterizations on the global
19 distribution of marine dimethyl sulfide, *J. of Geophys. Res.-Biogeo.*, 120, 2158–2177, doi:10.1002/2015JG003017, 2015.
- 20 Watanabe, Y. W., Yoshinari, H., Sakamoto, A., Nakano, Y., Kasamatsu, N., Midorikawa, T. and Ono, T.: Reconstruction of
21 sea surface dimethylsulfide in the North Pacific during 1970s to 2000s, *Mar. Chem.*, 103, 347–358,
22 doi:10.1016/j.marchem.2006.10.004, 2007.
- 23 Werdell, J., and Bailey, S.: An improved in-situ bio-optical data set for ocean color algorithm development and satellite data
24 product validation, *Remote Sens. Environ.*, 98, 122–140, doi:10.1016/j.rse.2005.07.001, 2005.
25
- 26 Whitney, F. A., Crawford, W. R., and Harrison, P. J.: Physical processes that enhance nutrient transport and primary
27 productivity in the coastal and open ocean of the subarctic NE Pacific, *Deep-Sea Res. Pt. II*, 52, 681–706,
28 doi:10.1016/j.dsr2.2004.12.023, 2005.
29
- 30 Wolfe, G. V., and Kiene, R.P.: Radioisotope and chemical inhibitor measurements of dimethyl sulfide consumption rates and
31 kinetics in estuarine waters, *Mar. Ecol. Prog. Ser.*, 99, 261–269, doi:10.3354/meps099261, 1993.
32

1 Wolfe, G. V., Strom, S. L., Holmes, J. L., Radzio, T. and Olson, B. M.: Dimethylsulfiopropionate cleavage by marine
2 phytoplankton in response to mechanical, chemical, or dark stress, *J. Phycol.*, 38, 948–960, doi:10.1046/j.1529-8817.2002.t01-
3 1-01100.x, 2002.
4

5 Wong, C., Wong, S., Richardson, W., Ith, G., Arychuk, M., and Page, J. Temporal and spatial distribution of dimethylsulfide
6 in the subarctic northeast Pacific Ocean: a high-nutrient–low-chlorophyll region, *Tellus* 57B, 317–331, doi:10.1111/j.1600-
7 0889.2005.00156.x, 2005.
8

9 Wu, X., Li, P., Liu, C., Zhang, H., Yang, G., Zhang, S., and Zhu, M.: Biogeochemistry of Dimethylsulfide,
10 Dimethylsulfiopropionate, and Acrylic Acid in the Changjiang Estuary and the East China Sea, *J. Geophys. Res.-Oceans*,
11 122, 10,245–10,261, doi:10.1002/2017JC013265, 2017.
12

13 Yoch, D. C.: Dimethylsulfiopropionate: its sources, role in the marine food web, and biological degradation to
14 dimethylsulfide, *Appl. Environ. Microbiol.*, 68, 5804–5815, doi:10.1128/AEM.68.12.5804-5815.2002, 2002.
15

16 Zeng, C., Rosengard, S. Z., Burt, W., Peña, A., Nemcek, N., Zeng, T., Arrigo, K. R., and Tortell, P. D.: Optically-derived
17 estimates of phytoplankton size class and taxonomic group biomass in the Eastern Subarctic Pacific Ocean, *Deep-Sea Res. Pt.*
18 *I*, 136, 107–118, doi:10.1016/j.dsr.2018.04.001, 2018.
19

20 Zindler, C., Peeken, I., and Marandino, C.: Environmental control on the variability of DMS and DMSP in the Mauritanian
21 upwelling region, *Biogeosciences*, 9, 1041–1051, doi:10.5194/bg-9-1041-2012, 2012.
22

23 Zubkov, M. V., Fuchs, B. M., Archer, S. D., and Kiene, R. P.: Rapid turnover of dissolved DMS and DMSP by defined
24 bacterioplankton communities in the stratified euphotic zone of the North Sea, *Deep-Sea Res. Pt. II*, 49, 3017–3038,
25 doi:10.1016/S0967-0645(02)00069-3, 2002.

26 Zubkov, M., Linn, L. J., Amann, R., and Kiene, R. P. Temporal patterns of biological dimethylsulfide (DMS) consumption
27 during laboratory-induced phytoplankton bloom cycles, *Mar. Ecol. Prog. Ser.*, 271, 77–86, doi:10.3354/meps271077, 2004.
28
29
30
31
32
33
34
35

1
2 **Table 1. Summary of DMS data included in this study. With the exception of the PMEL data, all measurements are derived from**
3 **membrane inlet mass spectrometry (MIMS).**

4

Cruise abbreviation	Vessel affiliation; cruise name and number	Sampling dates	Areal extent	Provinces included	No. data points	References
VIJ04	DFO; Central Coast BioChemical Study; 2004-24	12–19 Aug 2004	48° N - 52° N 131° W - 123° W	ALSK, CCAL	1913	(Nemcek et al. 2008)
LPJ07	DFO; Line P; 2007-13	1–16 Jun 2007	47° N - 55° N 146° W - 123° W	ALSK, CCAL, PSAE	21478	(Asher et al. 2011)
LPA07	DFO; Line P; 2007-15	16–30 Aug 2007	48° N - 54° N 146° W - 123° W	ALSK, CCAL, PSAE	16418	(Asher et al. 2011)
LPJ08	DFO; Line P; 2008-26	1–15 Jun 2008	48° N - 52° N 146° W - 123° W	ALSK, CCAL, PSAE	15304	(Asher et al. 2011)
LPA08	DFO; Line P; 2008-27	14–30 Aug 2008	48° N - 52° N 146° W - 123° W	ALSK, CCAL, PSAE	20881	(Asher et al. 2011)
VIJ10	DFO; La Perouse; 2010-12	1–4 Jun 2010	48° N - 52° N 130° W - 123° W	ALSK, CCAL	4551	(Tortell et al. 2012)
WCAC10	DFO; Ocean Acidification; 2010-36	22 Jul–15 Aug 2010	47° N - 57° N 138° W - 123° W	ALSK, CCAL, PSAE	25167	(Asher et al. 2017)
LPA11	DFO; Line P; 2011-27	19–28 Aug 2011	48° N - 51° N 146° W - 126° W	CCAL, PSAE	10802	(Asher et al. 2017)
LPA14	DFO; Line P and Strait of Georgia; 2014-19	29–31 Aug 2014	50° N - 51° N 145° W - 134° W	PSAE	2560	(Asher et al. 2015)
O16	UNOLS; Resolving DMS I: OC-1607A	12–27 Jul 2016	45° N - 56° N 143° W - 124° W	ALSK, CCAL, PSAE	18712	Previously unpublished
O17	UNOLS; Resolving DMS II: OC-1708A	12–27 Aug 2017	47° N - 57° N 146° W - 126° W	ALSK, CCAL, PSAE	10015	Previously unpublished
PMEL	various	various, 1984–2004	45° N - 61° N 167° W - 124° W	ALSK, CCAL, PSAE	3236	Various

1 Table 2. Summertime DMS data coverage across the NESAP region and within Longhurst provinces. Values indicate the number
2 of data-containing 1° x 1° spatial bins out of the total number of bins within the given area, with percent coverage of area shown in
3 parentheses. The left column represents the coverage for the PMEL data set (as utilized by L11) and the right column represents
4 the updated data set containing both PMEL measurements and MIM-based DMS concentration measurements.

5

Province Name	PMEL	This Study
CCAL	30/75 (40.0 %)	45/75 (60.0 %)
ALSK	61/119 (51.3 %)	83/119 (69.8 %)
PSAE	5/430 (12.8 %)	114/430 (26.5 %)
Total	126/1140 (11.1 %)	249/1140 (21.8 %)

6

7

1 **Table 3. Mean DMS concentrations, sea-air fluxes and total summertime DMS flux for the PMEL data set utilized by L11, and the**
 2 **updated data based used in this study.**

3

	PMEL			This Study		
Province	DMS (nM)	DMS Flux	Total summer DMS	DMS (nM)	DMS Flux	Total summer DMS
Name		($\mu\text{mol m}^{-2} \text{d}^{-1}$)	flux (Tg S)		($\mu\text{mol m}^{-2} \text{d}^{-1}$)	flux (Tg S)
CCAL	4.0 ± 0.5	4.4 ± 0.95	0.01	4.6 ± 0.4	6.3 ± 0.7	0.02
ALSK	8.9 ± 1.1	16.4 ± 4.0	0.06	7.5 ± 0.9	14.4 ± 3.0	0.05
PSAE	8.9 ± 0.7	21.0 ± 4.0	0.38	6.5 ± 0.4	16.5 ± 2.2	0.30
Total	7.2 ± 0.5	12.7 ± 2.0	0.32	6.2 ± 0.3	12.2 ± 1.4	0.30

4

5

1 Table 4. Pearson's correlation coefficients between DMS concentrations and other oceanographic variables binned to 1° spatial
 2 resolution. DMS data were derived from our combined PMEL and MIMS data set, variables derived from in-situ and satellite-
 3 based data. N represents the number of data pairs available for each correlation calculation. * indicates significance of $p < 0.05$.

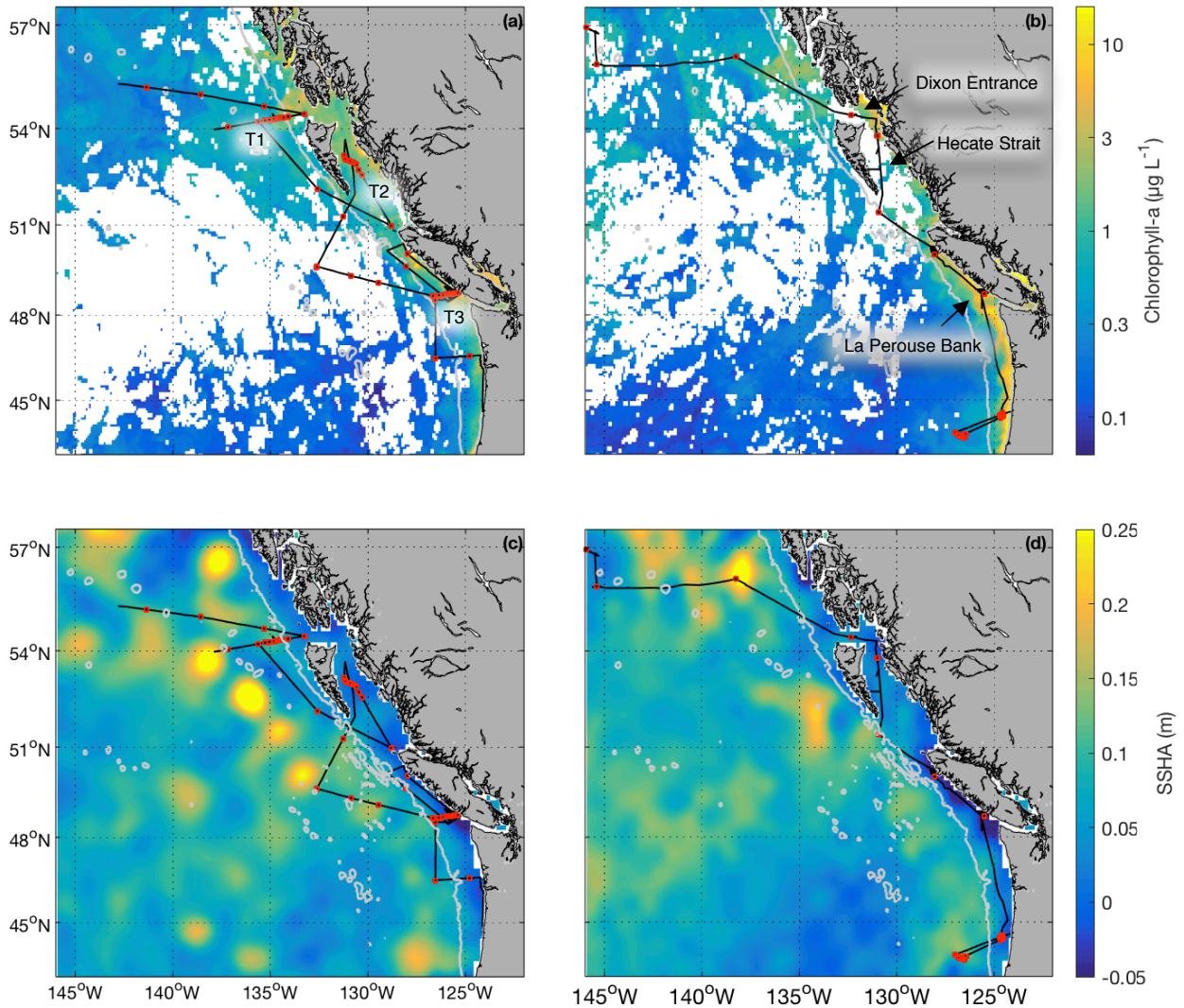
Variable	Whole region	CCAL	ALSK	PSAE
Salinity	$r = -0.04$	$r = 0.24$	$r = -0.04$	$r = 0.07$
	N = 223	N = 31	N = 83	N = 102
SST	$r = -0.01$	$r = -0.17$	$r = -0.32^*$	$r = 0.18$
	N = 248	N = 44	N = 83	N = 114
Chlorophyll- <i>a</i>	$r = 0.17^*$	$r = -0.11$	$r = 0.34^*$	$r = 0.45^*$
	N = 207	N = 31	N = 79	N = 99
Calcite	$r = 0.12$	$r = -0.08$	$r = -0.01$	$r = 0.50^*$
	N = 205	N = 30	N = 83	N = 99
PAR	$r = 0.04$	$r = -0.28$	$r = 0.41^*$	$r = 0.19$
	N = 212	N = 32	N = 52	N = 91
Depth	$r = -0.05$	$r = 0.20$	$r = -0.34^*$	$r = -0.02$
	N = 201	N = 45	N = 12	N = 96
MLD	$r = -0.14$	$r = 0.14$	$r = -0.06$	$r = -0.18$
	N = 98	N = 21	N = 11	N = 70
SSN	$r = 0.01$	$r = 0.14$	$r = 0.30^*$	$r = -0.18$
	N = 207	N = 31	N = 79	N = 99
SSHA	$r = -0.20^*$	$r = -0.34$	$r = -0.05$	$r = -0.47^*$
	N = 207	N = 30	N = 80	N = 102
NCP	$r = 0.22^*$	$r = 0.43^*$	$r = 0.05$	$r = 0.29$
	N = 91	N = 26	N = 25	N = 37
Wind	$r = 0.17^*$	$r = -0.06$	$r = 0.08$	$r = 0.29^*$
	N = 249	N = 45	N = 83	N = 114

4

5

Table 5. Pearson correlation coefficients and root mean square errors (nmol L⁻¹) between observed DMS concentrations and empirical predictions derived from the SD02, VS07 and W07 algorithms, using both published coefficients (original) and coefficients derived specifically for our NESAP observations using a least-squares approach (custom). Algorithm performance is shown for full NESAP region, as well as the three Longhurst biogeographic provinces within our study area. * indicates significance of p<0.05.

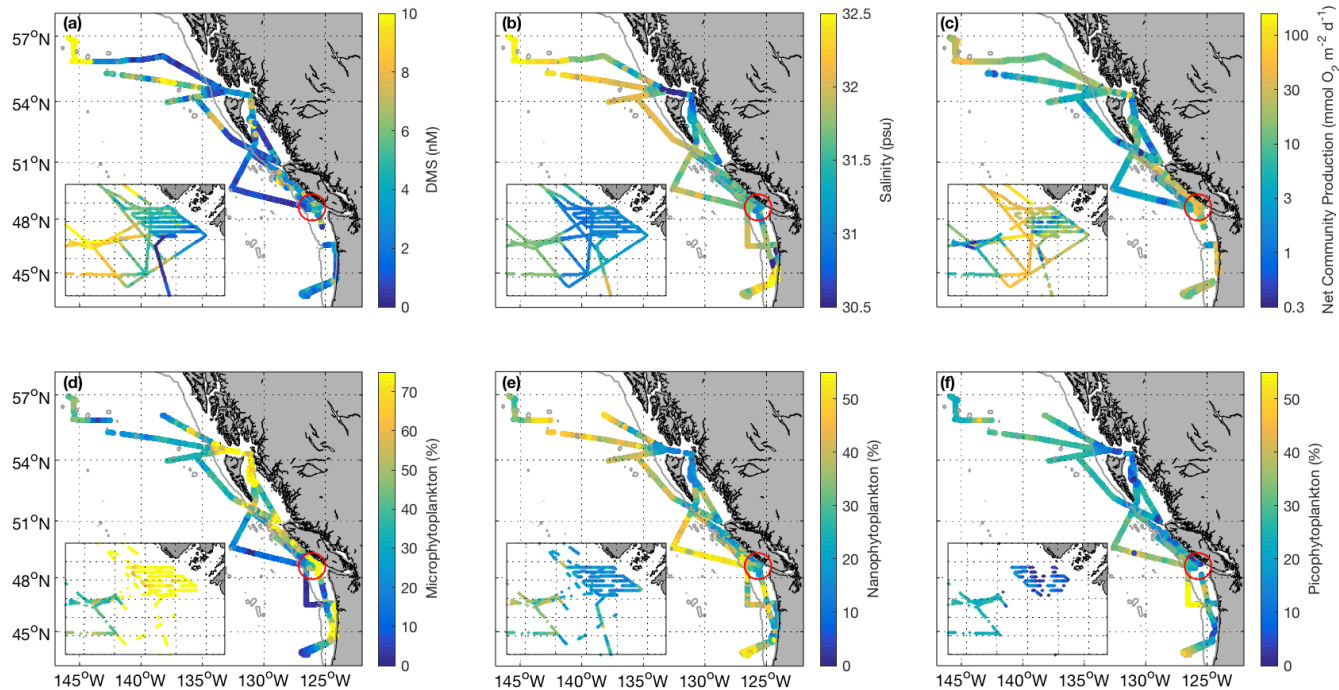
Province	SD02 original	SD02 custom	VS07 original	VS07 custom	W07 original	W07 custom	G18 original	G18 custom
Whole region	r = 0.05 RMSE = 3.77	r = 0.08 RMSE = 3.03	r = -0.31* RMSE = 4.95	r = 0.31* RMSE = 2.63	r = -0.08 RMSE = 67.1	r = 0.17* RMSE = 5.86	r = 0.19 RMSE = 3.1	r = 0.26* RMSE =
CCAL	r = 0.04 RMSE = 3.42	r = 0.62* RMSE = 1.61	r = -0.23 RMSE = 4.54	r = 0.23 RMSE = 1.20	r = -0.17 RMSE = 81.6	r = 0.27 RMSE = 2.04	r = 0.72* RMSE = 1.9	r = 0.69* RMSE =
ALSK	r = 0.16 RMSE = 2.37	r = 0.12 RMSE = 2.07	r = -0.10 RMSE = 3.43	r = 0.10 RMSE = 2.09	r = -0.20 RMSE = 47.5	r = 0.53* RMSE = 7.19	r = -0.41 RMSE = 3.4	r = 0.56 RMSE =
PSAE	r = 0.09 RMSE = 3.97	r = 0.23 RMSE = 2.94	r = -0.39* RMSE = 5.28	r = 0.39* RMSE = 2.81	r = -0.01 RMSE = 20.6	r = 0.44* RMSE = 4.59	r = -0.04 RMSE = 3.5	r = 0.26 RMSE =



2

3 **Figure 1. Cruise tracks and discrete sampling stations (red circles) for the July 2016 (O16) cruise (a,c) and August 2017 (O17) cruise**
 4 **(b, d). Panels (a) and (b) show chl-*a* concentration (log scale), derived from AquaMODIS satellite, and averaged over the duration**
 5 **of the respective cruise. Panels (c) and (d) show average sea surface height anomaly (SSHA). Panel (a) shows the location of the T1-**
 6 **T3 transects surveyed during the 2016, whereas panel (b) shows the geographic location of locations of interest. The grey line**
 7 **represents the coastal-oceanic boundary, defined here as the 2000 m isobath.**

8

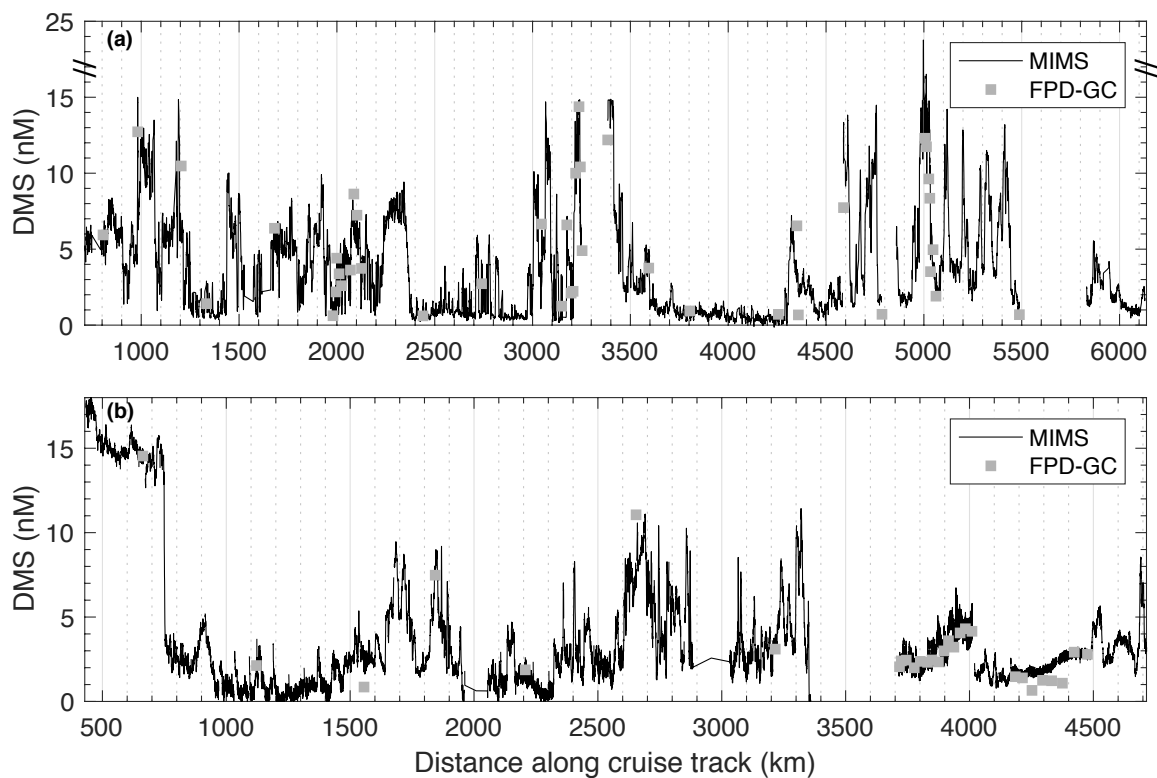


1

2

3 **Figure 2. Spatial distribution of DMS (a), salinity (b), net community production (C; note log scale), and micro-, nano-, and**
 4 **picophytoplankton relative abundance (d-f) during the O16 cruise July of 2016 and the O17 cruise August of 2017. Colour**
 5 **scaling on the maps are adjusted to ensure readability and best illustrate spatial patterns. Some data values are higher than the maximum**
 6 **scale of the colour bar. The inset box shows the La Perouse Bank region, as marked by the red circle. The grey line represents the**
 7 **coastal-open ocean boundary (2000 m isobath).**

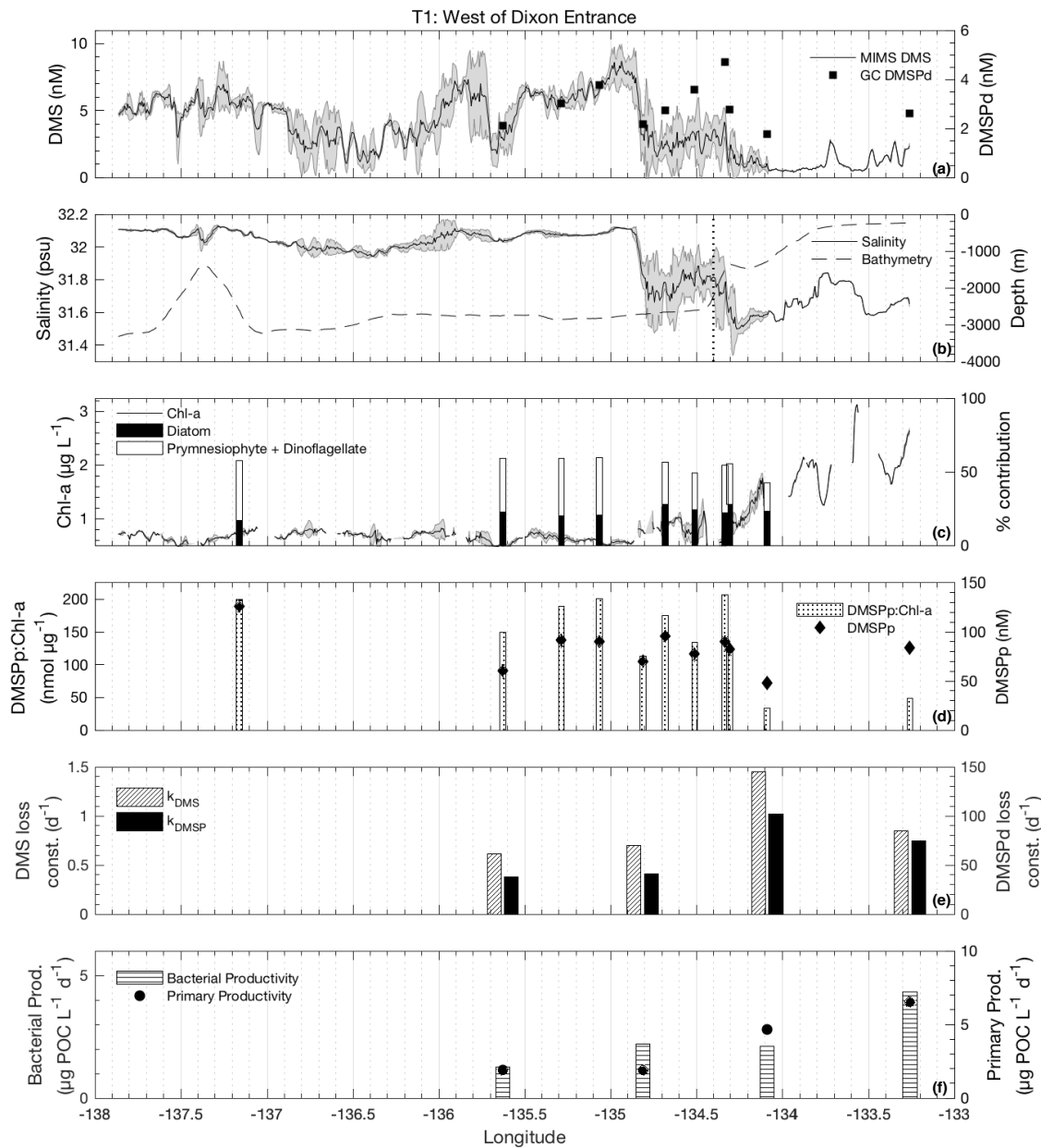
7



1

2 **Figure 3. DMS concentrations during the O16 cruise in July of 2016 (a) and the O17 cruise in August of 2017 (b) as measured by**
 3 **membrane inlet mass spectrometry (MIMS, continuous black line) and a purge-and-trap sampling system connected to a gas**
 4 **chromatograph equipped with a flame-photometric detector (grey symbols). Mean absolute error was 0.93 nM and root mean**
 5 **squared error was 1.4 nM for all paired measurements between the two instruments. A linear regression of the two data sets yields**
 6 **a coefficients of determination of $r^2=0.89$.**

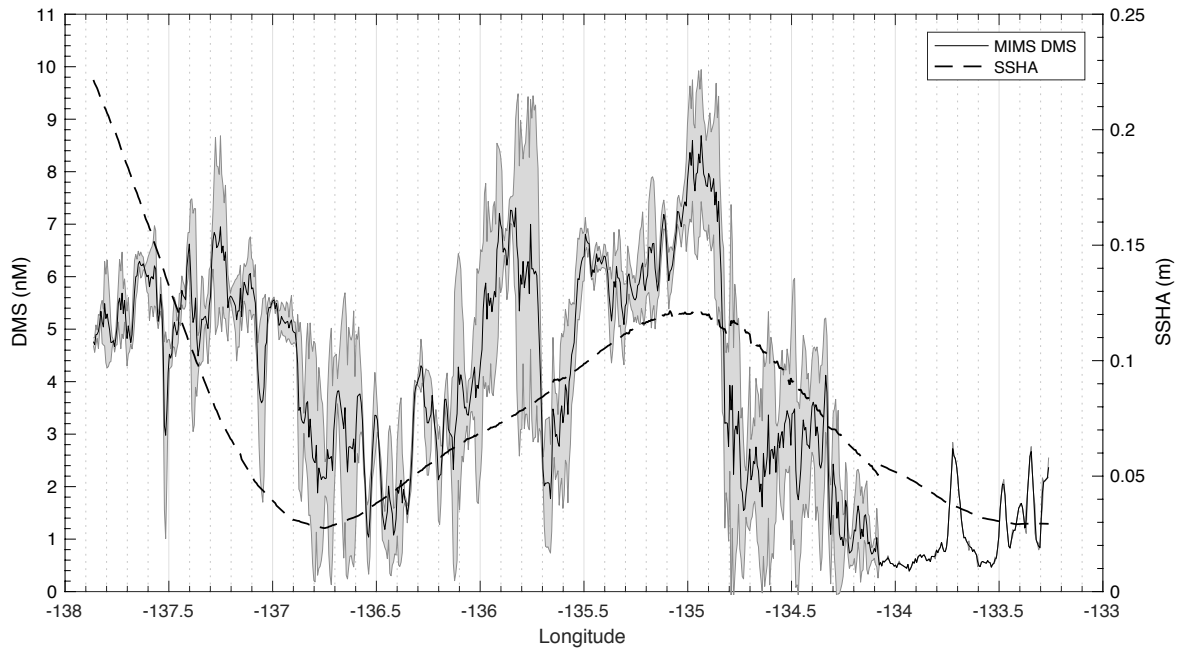
7



1

2 **Figure 4.** MIMS-based DMS concentration measurements and station-based DMSPd measurements (a), salinity and bathymetry
 3 (b), chl-*a* and HPLC-based station estimates of diatom and prymnesiophyte as defined % contribution to total assemblage (c),
 4 **DMSPp concentrations and DMSPp:chl-*a* ratios** (d), DMS/P consumption rate constants (e), and bacterial and primary productivity
 5 rates (f) along the T1 transect west of Dixon Entrance during July 2016 (O16 cruise). Shaded regions represent standard deviation
 6 of repeated measurements across the transect. The vertical dotted line in panel (b) indicates the approximate shelf break (2000 m),
 7 at 134.4° W.

1



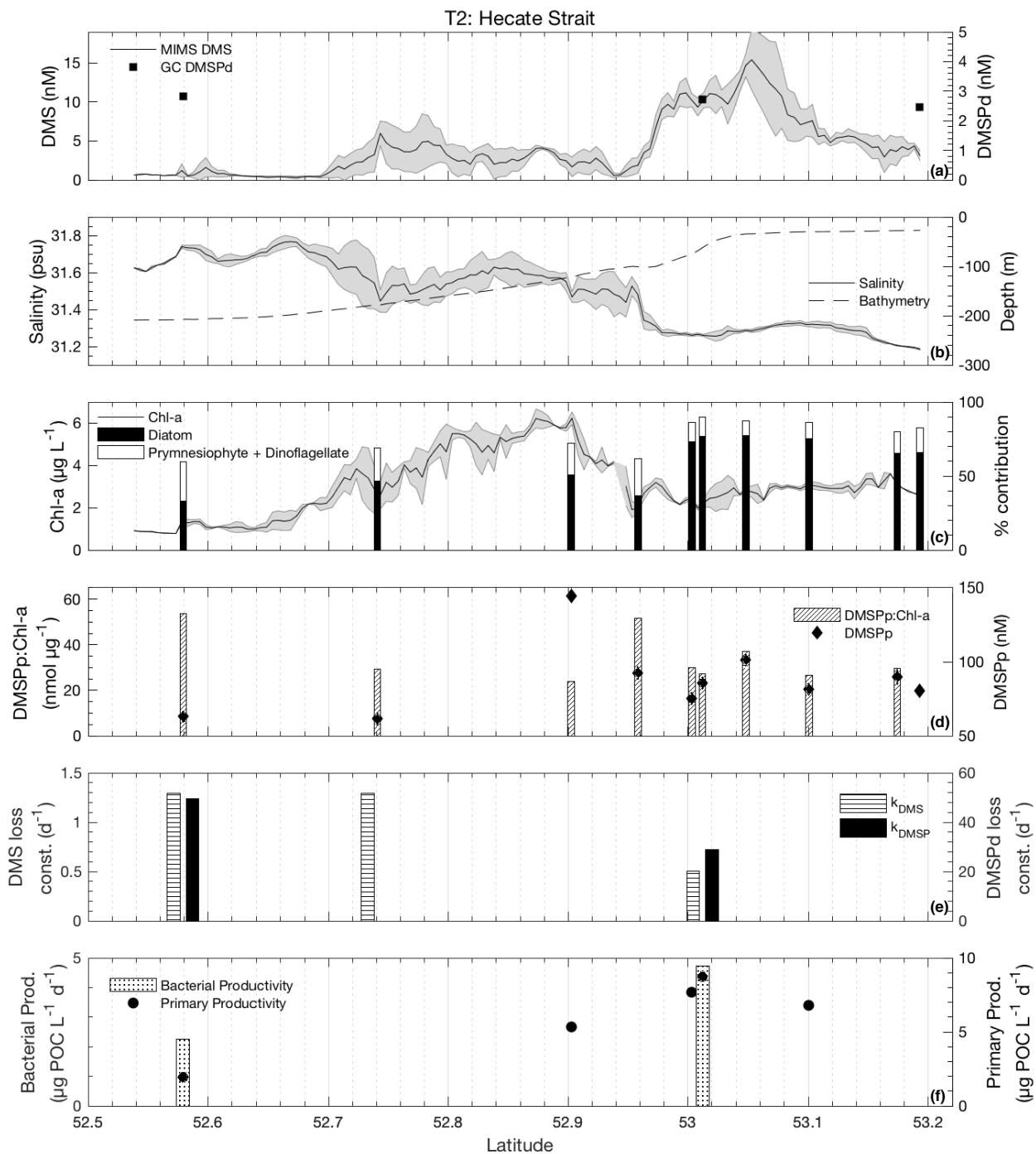
2

3 **Figure 5. Line plot of sea surface height anomaly (SSHA) on 15 July, 2016 and observed DMS concentrations between 14 July and**
4 **16 July, 2016 along T1. DMS along the T1 transect is highest in those areas influenced by positive SSHA values.**

5

6

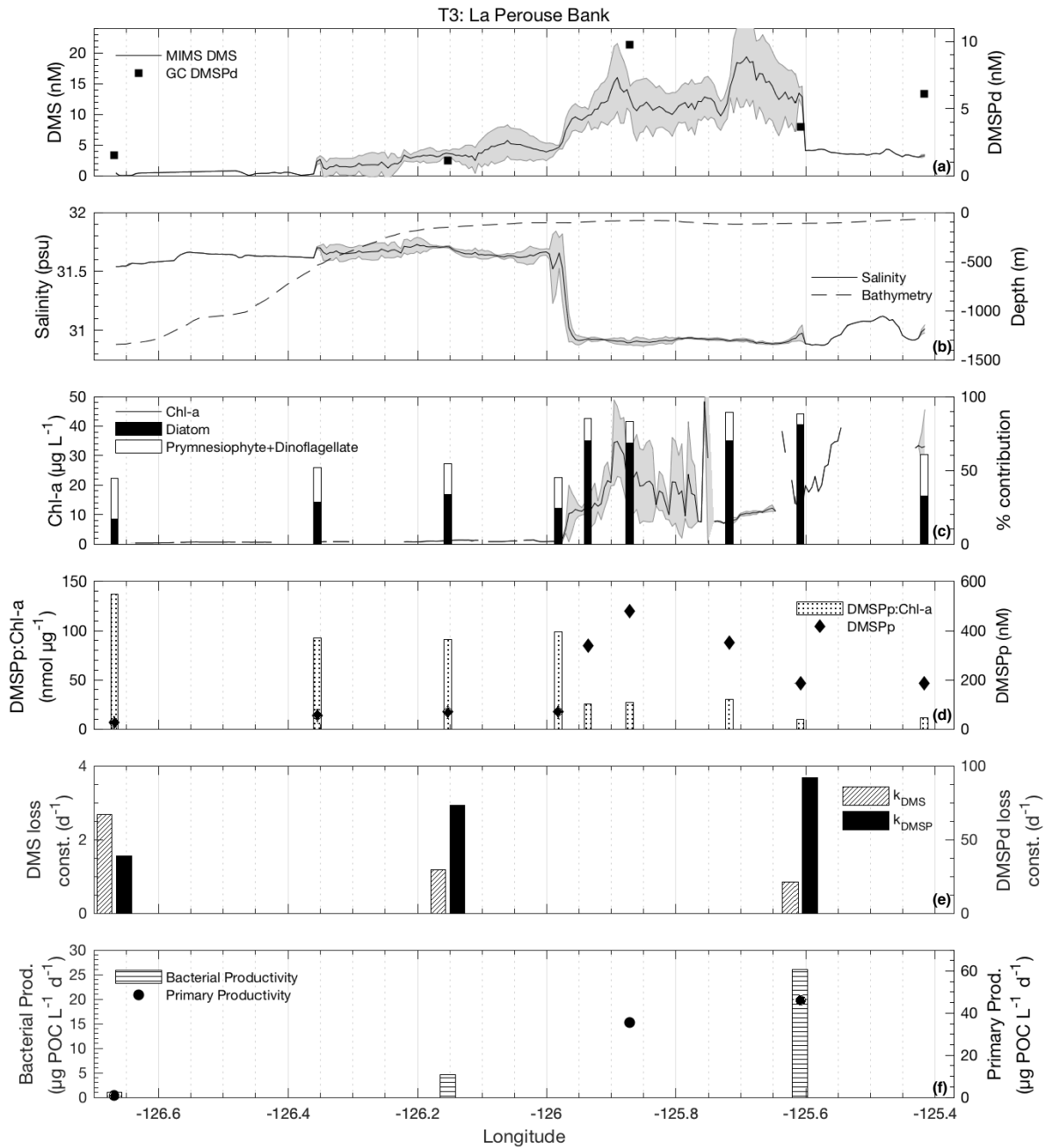
7



1

2 **Figure 6.** As for Fig. 4, but for the T2 transect.

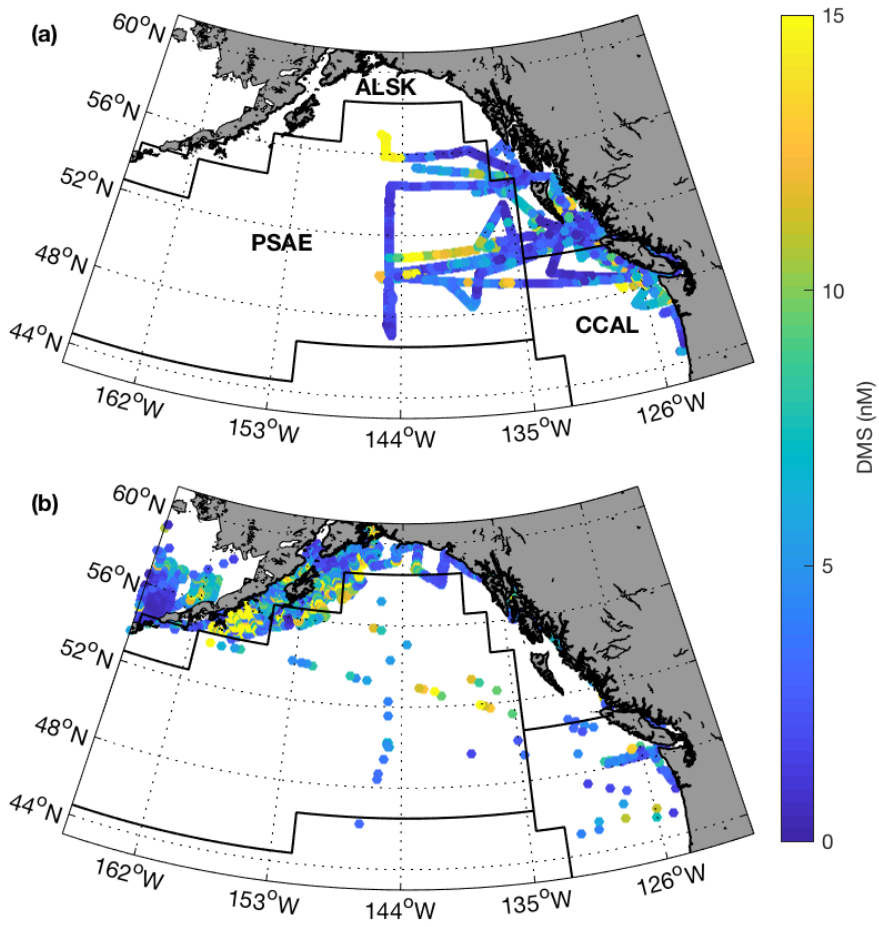
1
2



3

4 **Figure 7.** As for Figs. 4 and 6, but for the T3 transect.

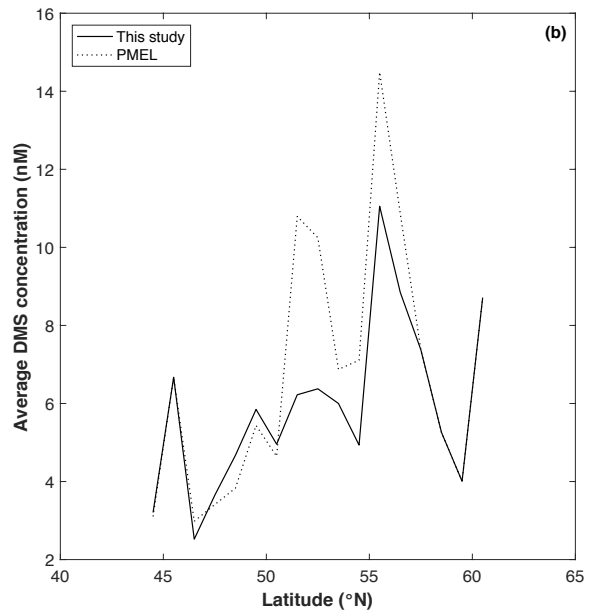
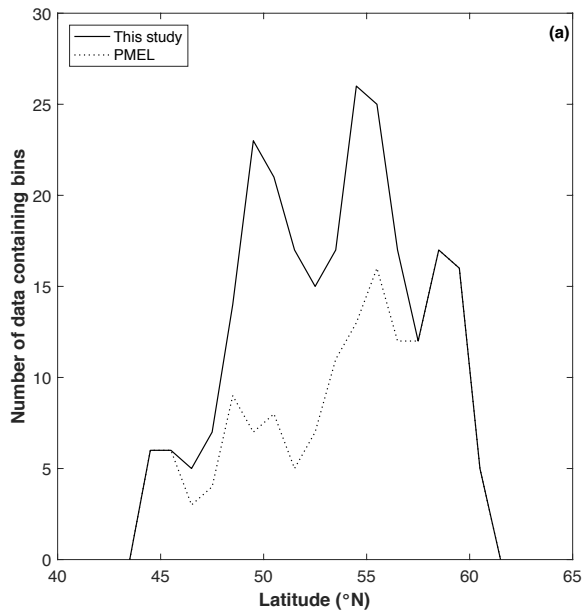
1



2

3 **Figure 8. Spatial distribution of summertime DMS measurements from MIMS (a; 2004-2017) and the PMEL (b; 1984 - 2004) data**
4 **set. Black lines represent boundaries of Longhurst biogeographical provinces, with province names show in panel (a).**

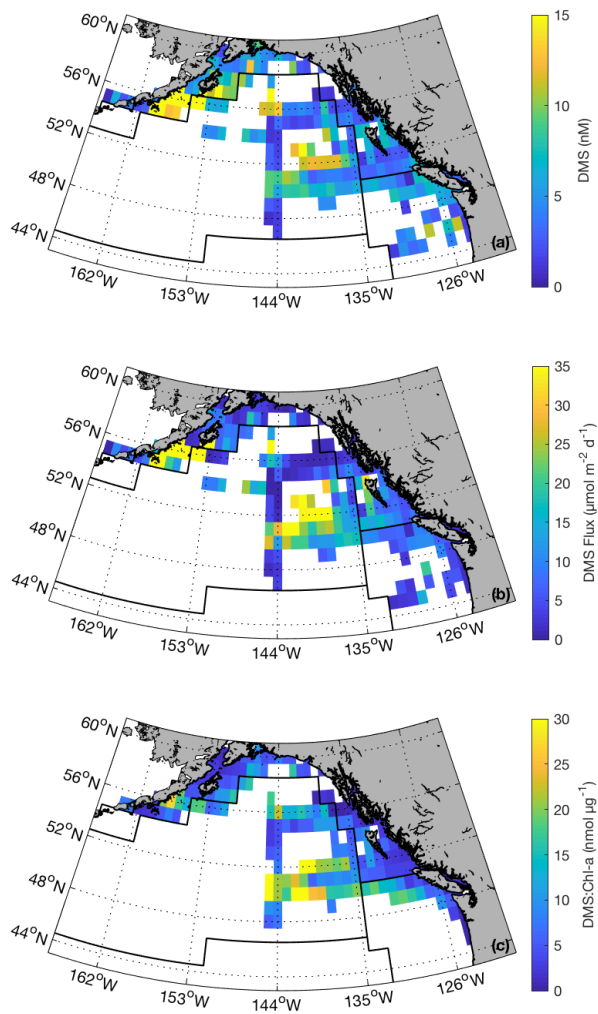
5



1

2 Figure 9. Latitudinal distribution of data-containing bins (a) and average DMS concentration (b) for PMEL (dotted line) and
 3 combined (PMEL and MIMS) data sets.

4



1

2 **Figure 10. Summertime DMS concentrations (a), DMS sea-air fluxes (b), and DMS:chl-*a* ratios (c) binned to 1° x 1° spatial**
 3 **resolution. These maps were derived using our combined PMEL/MIMS data set (1984–2017; June, July and August). Black lines**
 4 **correspond to boundaries of Longhurst biogeochemical provinces (see Fig. 8 for province names). Maximum values (47 nM, 180**
 5 **$\mu\text{mol m}^{-2} \text{d}^{-1}$, and 47 $\text{nmol } \mu\text{g}^{-1}$ for panels a, b, and c, respectively) exceed the bounds of the colorbars. Maximum values for DMS**
 6 **and DMS flux occur in the waters south of the Alaska Peninsula, whereas maximum DMS:chl-*a* occurs mid PSAE.**

7